Recovery of benthic communities following the Toarcian oceanic anoxic event in the Cleveland Basin, UK

Bryony A. Caswell[a, b*] and Stephanie J. Dawn[c]

Affiliations: [a]Environmental Futures Research Institute, Griffith University, Gold Coast Campus, Parklands Drive, Queensland 4222, Australia; [b]Department of Geography, Geology and Environment, University of Hull, Hull, HU6 7RX, UK; [c]School of Environmental Sciences, University of Liverpool, Brownlow Hill, Liverpool, L69 3GP, United Kingdom.

***Corresponding author:** b.a.caswell@hull.ac.uk; Tel: +61755529189

Word count = 7828

Figure captions = 777

References = 3866

Figures = 5 (plus 2 supplementary)

Tables = 3 (plus 3 supplementary)

Abstract

During the Toarcian oceanic anoxic event (OAE) considerable environmental changes occurred that were associated with global warming, perturbations to the C-cycle and ocean deoxygenation which resulted in a mass extinction of marine fauna. Recovery of the biota after the event was protracted and has to date undergone limited study. However, understanding the patterns and processes of recovery are critical to anticipating ecosystem responses to the environmental changes predicted for the near future. Results showed that increases in benthic diversity, and the re-establishment of the Toarcian infauna was gradual and followed the changing redox conditions. Pioneering infauna, such as *Dacryomya ovum* that dominated the

©2020, Elsevier. This manuscript version is made available under the CC-BY-NC-ND 4.0 license http://creativecommons.org/licenses/by-nc-nd/4.0/

seafloor after the event in the Cleveland Basin, Yorkshire, UK, can modify the physico-chemical environment and thus facilitate ecological succession after disturbance. The length of *D. ovum* increased >8 mm throughout the *bifrons* Zone and these body-size changes were linked with total organic carbon (TOC) content suggesting a link to primary productivity, although only at intermediate levels of deoxygenation. Major changes in the phytoplankton, and so food supply, seem to have driven changes in bivalve body size, across trophic guilds, both during and after the event in Yorkshire, and on the mid to lower shelf in Spain and France, respectively. Primary productivity collapse seems then to have been a major driver of biotic change throughout the Toarcian event, as it was during the Permian–Triassic, Triassic/Jurassic and Cretaceous/Tertiary mass extinctions. Further investigation of both the palaeontological and geochemical changes that occurred within early successional Toarcian infaunal communities are required to more fully understand the pattern of recovery after the OAE.

Keywords: Jurassic; Lilliput effect; shell morphology; population structure; dysoxia; Alum Shale Member

1. Introduction

In early Toarcian (~183 Ma) global warming occurred, recorded as a 7–13˚C increase surface ocean temperatures (Bailey et al. 2003; Gomez and Arias 2010; Korte et al. 2015; Suan et al. 2008) which was associated with increases in atmospheric pCO_2. Large negative carbon isotope excursions are recorded in marine organic matter, marine carbonates, fossil plants and wood across the northern (Caruthers et al. 2011; Kemp et al. 2005; Hermoso et al. 2009a, Hesselbo et al. 2007, Hesselbo and Pienkowski 2011, Röhl et al. 2001; Ullmann et al. 2014) and southern hemispheres (Al-Suwaidi et al. 2010; Gröcke et al. 2011; Kemp and Izumi 2014). The warming

©2020, Elsevier. This manuscript version is made available under the CC-BY-NC-ND 4.0 license http://creativecommons.org/licenses/by-nc-nd/4.0/

56 was accompanied by sea level rise (Haq, 2017; Hesselbo and Jenkyns 1998),
57 increased rates of continental weathering (Cohen et al. 2004) and changes in the
58 patterns of ocean primary productivity (Jenkyns 2010) which triggered an oceanic
59 anoxic event (OAE).

60 Contemporaneous global ocean deoxygenation (N. B. encompassing both
61 hypoxia (1-30% of saturation) and anoxia (absence of oxygen)) is indicated by the
62 enhanced widespread deposition of marine organic carbon (Jenkyns 1988), and
63 changes in proxies for seawater redox (Pearce et al. 2008; Thibault et al. 2018)
64 although the extent of the deoxygenation varied geographically (Hermoso et al.
65 2009b; Kemp and Izumi 2014; Rodriguez-Tovar and Reolid 2014). Early Toarcian
66 ocean deoxygenation is linked with a mass extinction of marine life (Caswell et al.
67 2009; Little and Benton 1995, Little 1996), biogeographic range shifts of key taxa
68 (Caswell and Coe 2014; Dera et al. 2011; Nikitenko et al. 2008), and large shifts in
69 seafloor community composition (Caswell and Frid 2017; Danise et al. 2013; Danise
70 et al. 2015) and the body size of taxa that dominated the seafloor during the OAE
71 (Caswell and Coe 2013). Large decreases in the amount of dissolved oxygen in the
72 oceans have occurred over the last 60 years as a consequence of global warming
73 and anthropogenic nutrient inputs (Diaz and Rosenberg 2008; Stramma et al. 2010);
74 and models predict a continued decline of up to 7% over the next century (Keeling et
75 al. 2010). The ecological changes that occurred during the Toarcian are
76 commensurate with the mass mortalities (Breitburg et al. 2018; Falkowski et al.
77 1980), changes in organism behaviour (Gray et al. 2002; Riedel et al., 2014; Seitz et
78 al. 2003), growth rates and body size (Caswell and Coe 2013; Cheung et al. 2013)
79 that are occurring in deoxygenated areas today.

80

81 During the early Toarcian the seafloor in NW Europe was dominated by the
82 epifaunal suspension feeding bivalves *Bositra radiata* and *Pseudomytiloides dubius*

©2020, Elsevier. This manuscript version is made available under the CC-BY-NC-ND 4.0 license http://creativecommons.org/licenses/by-nc-nd/4.0/

before and during the OAE (*Dactylioceras tenuicostatum* and *Harpoceras exaratum* ammonite subzones), respectively, which underwent large shifts in abundance and body size during the event (Caswell et al. 2009, Röhl et al. 2001). Changes in the size of these species have been linked to changes in primary production (Caswell and Coe 2013). Although we now know how some Toarcian marine communities changed during the event (Caswell and Coe 2013; Clemence et al. 2015; Danise et al. 2013; Fürsich et al. 2001; Gomez and Arias 2010; Röhl et al. 2001), we know comparatively little about the faunal changes that occurred during the recovery from the OAE (which is geochemically defined as the *exaratum* Subzone; Pearce et al. 2008). The present study considers changes in the benthic communities, of the Cleveland Basin, Yorkshire, UK, in the aftermath of the OAE (*Dactylioceras bifrons* ammonite Zone). The benthos remained impoverished for a considerable period, requiring >900 kyr for the infauna to return (Caswell and Frid 2017), despite the somewhat improved conditions, as indicated by a suite of geochemical proxies (Cohen et al. 2004; Hesselbo et al. 2000; Kemp et al. 2005; Kemp et al. 2011; Pearce et al. 2008; Raiswell et al. 1993).

The post-OAE seafloor communities were of low diversity and were dominated by the nuculanid bivalve *Dacryomya ovum* (Sowerby) in the *bifrons* Zone. This was the first infaunal taxon to occur in abundance after the OAE in the Cleveland Basin, i.e. specimens of the infaunal brachiopod *Lingula longovicensis* and the bivalve *Goniomya rhombifera* occur briefly (at the top of Beds 38 and 48, respectively; bed numbering after Howarth 1962; Caswell et al. 2009) but are not abundant. *D. ovum* occurs abundantly in the UK within Toarcian organic-rich mudrocks (Hesselbo and Jenkyns 1995; Horton and Edmonds 1987; Little 1996; Martin 2004; Morris 1979; Watson 1982). Nuculanids with strong taxonomic affinities to *D. ovum* occur in coeval organic-rich strata worldwide, including: *Dacryomya*

©2020, Elsevier. This manuscript version is made available under the CC-BY-NC-ND 4.0 license http://creativecommons.org/licenses/by-nc-nd/4.0/

lacrymya in the Toarcian Schistes Cartons, France (Fürsich et al. 2001), *Nuculana (Praesaccella) ovum* in Sinemurian–Toarcian facies in Spain (Gahr 2002), Chile, Argentina (Aberhan 2002; Damborenea 1987) and British Columbia (Aberhan 1998). *Dacryomya* spp. Also occurred in Toarcian successions in Russia and Siberia (Nikitenko and Shurygin 1992; Shurygin 1983; Zakharov et al. 2006).

Organism body-size affects fundamental physiological, ecological and evolutionary processes. For example, organism life history, metabolic rates, the geographic range and extinction rates of organisms all scale disproportionately with body mass (Smith and Lyons 2013). Notable decreases in body-size have been recognised after at least six extinctions (Girard and Renaud 1996, Gobbett 1973; Harries 1993; Håkansson and Thomsen 1999; Kaljo 1996, Ward et al. 2004) including the early Toarcian (Caswell and Coe 2013, Voros 2002) when organisms of small, or stunted, size dominate which is thought to be a phenotypic reaction to unfavourable growth conditions (known as the 'Lilliput effect'; Urbanek 1993).

Bivalve intraspecific shell morphology has also been shown to vary with deoxygenation. For instance, in the Baltic Sea the normally suborbicular shells of *M. balthica* become elongated with a flexed posterior end which correlates with increasing hypoxia, and has been linked with siphon extension above the redox boundary (Sokołowski et al. 2008). Fossil *D. ovum* have a similar elongated (or 'rostrate') posterior and we hypothesise that variations in the degree of elongation could have helped *D. ovum* to colonise the seafloor after the Toarcian OAE.

Infaunal taxa, such as *D. ovum*, can act as ecosystem engineers (Jones et al. 1994) in that they alter the physicochemical environment by burrowing: their bio-irrigation of the sediment increases oxygenation, redistributes sediment particles,

©2020, Elsevier. This manuscript version is made available under the CC-BY-NC-ND 4.0 license http://creativecommons.org/licenses/by-nc-nd/4.0/

organic material, minerals and microbes; in the process sedimentary structures and biogeochemical gradients are created (Welsh 2003). Sediment mixing increases the habitable area available to taxa that are intolerant of low oxygen (Meysman et al. 2006); and, the creation of biogeochemical gradients affects the sedimentary fluxes of nutrients in to the water column stimulating primary productivity (Graf and Rosenberg 1997; Jørgensen et al. 1995; Kristensen 2000). The increased sediment heterogeneity and habitat complexity stimulates biodiversity. So, the appearance of infaunal bivalve populations after the OAE would have been an important step in the recovery of the seafloor communities.

This study aims to determine the patterns of change within the benthic communities of the *bifrons* ammonite Zone during the recovery from the Toarcian OAE. The development of early successional benthic communities dominated by *D. ovum* (usually monospecific) were investigated in terms of their taphonomy, palaeoecology, morphometry and life history from sections near Whitby, North East Yorkshire, UK. Changes in Yorkshire are considered for both *D. ovum* populations and the whole benthic macrofaunal community.

2. Methods

2.1 Geological setting

The lower Jurassic succession was deposited in the Cleveland Basin, Yorkshire, UK that extends into the Sole Pit Trough of the North Sea Basin (Fig. 1). The 71 m thick lower Toarcian Whitby Mudstone Formation was deposited in a semi-restricted fully marine basin below storm wave base, and the lithology is typical of the organic-rich mudrocks that were deposited across NW Europe at that time (Jenkyns 1988, Jenkyns 2010, Hesselbo and Jenkyns 1995). It is one of the most complete and expanded exposures of the Late Pliensbachian – Early Toarcian period in the world (and includes the Global Boundary Stratotype Section and Point for the base of the

©2020, Elsevier. This manuscript version is made available under the CC-BY-NC-ND 4.0 license http://creativecommons.org/licenses/by-nc-nd/4.0/

Pliensbachian Stage). The formation is biostratigraphically subdivided into five ammonite zones described in detail by Howarth (1955, 1962, 1973, 1992).

2.2 Field data collection

Populations of the bivalve *Dacryomya ovum* (Sowerby) were sampled throughout the organic-rich facies of the Whitby Mudstone Formation between Whitby (54°29'28.48"N, 0°36'33.89"W) and Saltwick Bay (54°31'15.84"N, 00°35'15.68"W), NE Yorkshire, UK (Figs 1, 2A–H). Approximately 30 m of vertical section, from the upper 3 m of the Mulgrave Shale Member to the lower 27 m of the Alum Shale Member (upper *Harpoceras falciferum* to *Catacoeloceras crassum* ammonite subzones; Fig. 3), were sampled from bedding planes in the foreshore exposures and sea cliffs. Benthic macrofossil presence and absence data were collected approximately every 0.5m. Data and samples for morphometric analyses were collected from 30 discrete levels throughout the range of *D. ovum* (where it occurred in abundance). Each observation/sample was precisely located relative to known stratigraphic datums based on Howarth (1962).

At each of the 30 stratigraphic levels the following information was recorded: *D. ovum* abundance, the shell orientation within the bedding (e.g. parallel, orthogonal or oblique), and the compass orientation of the posterior end relative to the azimuth. At each level all fossils were marked and bedding planes were photographed at high resolution for spatial analyses of shell clustering. Subsequently, all body fossils were extracted from each level for later measurement in the laboratory. The spatial clustering of shells within each bedding plane was determined from field photographs using the nearest neighbour statistic, R, from the method of Hammer and Harper (2006) where $R = \frac{d}{0.5 \times \left(\frac{a}{n}\right)}$ and *d* is the mean distance of each object from its nearest neighbour, *a* is the total area surveyed, and *n* is the total number of objects. Clustering was indicated by R≤1.00 and dispersal by R≥1.01.

©2020, Elsevier. This manuscript version is made available under the CC-BY-NC-ND 4.0 license http://creativecommons.org/licenses/by-nc-nd/4.0/

192

193 **2.3 Shell morphometrics and growth**

194 Shell height, length and inflation were measured (Fig. 2A and 2H) for all
195 extracted body fossils (n = 629) to the nearest 0.01 mm using digital Vernier
196 callipers. The shell height and length of external moulds (n = 206) were measured in
197 the field. For the small number of disarticulated specimens (n = 15), shell inflation
198 was measured from a single valve and doubled. Ratios of shell height: shell inflation
199 were calculated, for all extracted fossils, to provide an index of the degree of *post*
200 *mortem* lateral shell compaction (e.g. Fig. 2F–G). Population size structure was
201 explored using the length frequency distributions (LFDs).

202

203 To investigate variations in shell shape between the different assemblages
204 high-resolution photographs were taken of the exteriors of all extracted right valves
205 (complete fossils and internal moulds; n = 633). For the disarticulated specimens
206 (2% of shells collected) both the left and right valves were measured. Fifteen
207 measurements were made (Fig. 2A) from each fossil using the measure and angle
208 tools (the latter to delineate the 14 dorso-ventral measurements) in Image J
209 (version 1.49m, NIH) on calibrated photographs and three indices to describe shell
210 shape (derived by Sokolowski *et al*. 2008) were calculated, as follows.

211

212 $$SDI1 = \frac{((UV + US))/2}{(UE + UF + UG + UH + UI)/5} \quad \textbf{(1)}$$

213

214 $$SDI2 = \frac{(UJ + UK)/2}{(UE + UF + UG + UH + UI)/5} \quad \textbf{(2)}$$

215

216 $$SDI3 = \frac{UV + US}{UJ + UK} \quad \textbf{(3)}$$

©2020, Elsevier. This manuscript version is made available under the CC-BY-NC-ND 4.0 license http://creativecommons.org/licenses/by-nc-nd/4.0/

SDI1 describes the flexure of the posterior shell margin (low values indicate high flexure), and SDI2 compares the symmetry of the posterior and anterior shell margins (low values indicate greater asymmetry). SDI3 describes the differences in shell elongation between the posterior and anterior end (low values indicate greater elongation of the posterior).

External growth rings were counted for six complete valves of *D. ovum* (from four assemblages) and the distances between them were measured along the axis of maximum growth. Annuli were identified on the basis of their morphological distinctiveness (boldness, colour, topography and continuity across the shell surface) when examined under a light source. Using the shell height at age data and the software Fishparm v.3 (Prager et al. 1994) shell growth was modelled using the von Bertalanffy growth function $H_t = H_\infty \left(1 - e^{-k\,(t - t_0)}\right)$ (Jones et al. 1989; von Bertalanffy 1938). Where, t = age (years), H_t = shell height at age t, H_∞ = maximum shell height, K = growth constant and t_0 = age when H = 0. Using the growth constant, an omega value (ω), indicative of population growth rate, was derived from $\omega = kH_\infty$ (Carroll et al. 2011).

2.4 Data analysis

Changes within the *D. ovum* assemblages are considered within the context of the whole benthic community using data on body fossil occurrences from Little (1995, 1996) and Caswell et al. (2009), and data on trace fossils from Martin (2004). The relationships between biotic variables were explored using reduced major axis linear regression using Past.exe (Hammer and Harper 2001, 2006). The relationships between shell morphometrics and palaeoenvironmental changes were explored using stepwise multiple regression (SPSS v. 21) with geochemical proxy

©2020, Elsevier. This manuscript version is made available under the CC-BY-NC-ND 4.0 license http://creativecommons.org/licenses/by-nc-nd/4.0/

data for primary production (TOC; from Cohen et al. 2004 and Harding 2004), palaeoredox ([Mo], [U], TOC/TS; from Harding, 2004, Pearce et al. 2008 and McArthur et al. 2008) and surface seawater temperature ($\partial^{18}O_{belemnite}$; from McArthur et al. 2008 and Ullman et al. 2014; proxy data for benthic water temperatures being unavailable). The multiple regressions were performed on the complete data and subsets of the data subdivided based on the median TOC content (2%). Using subsets of the data allowed us to account for changes in the response of environmental drivers under different redox conditions. The differences between biotic parameters were explored between the different assemblages and the two categories (≤ 2% and ≥ 2%) of TOC using nonparametric tests such as the Kruskal-Wallis, Jonckheere-Terpstra and Mann Whitney U-test (using SPSS v. 21).

Fossil preservation varied stratigraphically: in assemblages below 49.4m almost all fossils were preserved as complete body fossils and above 49.4m they were preserved as internal moulds (Supplementary Table S1). To explore changes in body size and shape through time these data had to be pooled. The measurements for fossils preserved as internal moulds might be expected to underestimate the actual body-size due to the lack of a shell. Therefore interpretations of the size differences between assemblages comprised entirely of body fossils (with shell) and those comprising internal moulds underestimate the true size difference between these stratigraphic levels by ~3 mm (the measured shell thickness).

3. Results

3.1 Taphonomy of *Dacryomya ovum* assemblages

Within the Alum Shale Member *D. ovum* occurs in matrix supported shell pavements. Most occurrences were monospecific except for pyritised trace fossils that were present at some levels (Fig. 4). Most *D. ovum* were preserved as complete

©2020, Elsevier. This manuscript version is made available under the CC-BY-NC-ND 4.0 license http://creativecommons.org/licenses/by-nc-nd/4.0/

body fossils (54%), a further 30% were preserved as internal moulds and 16% as external moulds. Only 2% of shells were disarticulated into their separate valves. Although 20% of fossils showed some fractures (Supplementary Information Table S1; Fig. 2) the majority were undamaged. *D. ovum* preservation varied through time: between 38.00 and 49.35 m most shells were preserved as body fossils, and above 49.47 m most were preserved as internal moulds (Supplementary Information Table S1). This suggests that the factors influencing preservation changed in the lower *Peronoceras fibulatum* Subzone.

The body fossils were comprised of shell material, most were filled with the mudrock matrix and some had a thin layer of pyrite coating the inner shell surface. One specimen from 51.22 m had the inarticulate brachiopod *Discinisca infraoolithica* attached to the outer surface, but there was no evidence for boring or other epibiont overgrowth. The nature of the shell pavements and the lack of disturbance (e.g. disarticulation, shell breakage, and epibiont overgrowth) suggest the *D. ovum* pavements are autochthonous or parautochthonous assemblages representing biogenic concentrations of fossils in near-life position.

3.1.1 Shell compaction

Un-compacted *D. ovum* shells are naturally inflated with a rostrate posterior end (which is typical of the genus; Table 3, Fig. 2A-B) the extent of which varied between individuals (Fig. 2B–E). Most inflated *D. ovum* specimens without visible signs of compaction had shell height/inflation (h/i) ratios between 1.1 and 1.3 (Fig. 2B–E), shells with some evidence of compaction (e.g. shell fractures and collapsed areas) had ratios of 1.4–2.73 (Fig. 2F–G), and shells which appeared highly compacted had ratios >2.73. Of all specimens measured 20% were uncompacted, 50% were moderately compacted and the remaining 30% were significantly

©2020, Elsevier. This manuscript version is made available under the CC-BY-NC-ND 4.0 license http://creativecommons.org/licenses/by-nc-nd/4.0/

297 compacted. Shell height/inflation was not correlated with shell length, height, nor the
298 three shape ratios (reduced major axis linear regression p>0.05). Thus, the lateral
299 compaction of shells, as indicated by shell height/shell inflation, does not seem to
300 have influenced these morphometric parameters. Examination of the specimens
301 showed that one valve was usually inflated whereas the other collapsed and
302 fractured under compression (Fig. 2F). *D. ovum* shell height/inflation decreased
303 throughout the section (Fig. 3A; linear regression, $R^2 = 0.52$, $F = 29.73$, $p<0.001$)
304 meaning shells were more compacted in the lower part of the section.

305

306 ***3.1.2 Spatial distribution of fossils within shell pavements***

307 Shells were concordant (e.g. parallel), oblique and perpendicular to the
308 bedding. However, in most *D. ovum* assemblages (67%) shells were concordant. At
309 five stratigraphic levels ≥50% of fossils were oblique or perpendicular to the bedding.
310 These shells were considered to be in an infaunal life position within the sediment,
311 and so represented an autochthonous assemblage. Bivalve shells that have rostrate
312 posterior ends, like *D. ovum*, tend to live with the long-axis oriented vertically with the
313 posterior projected towards the sediment surface (Stanley 1970, Stanley 1981).
314 Shells that were concordant with the bedding may be parautochthonous or may
315 reflect differences in living habit between assemblages due to environmental
316 changes.

317 Nearest neighbour analyses showed that in 12 of the shell pavements shells
318 were clustered (R = 0.32 to 0.98) within the bedding plane, and in the other 17 they
319 were dispersed (R = 1.02 to 2.86; Fig. 4), and there was no trend through time
320 (linear regression $R^2 = 0.025$, $F = 0.73$, $p = 0.40$). At most stratigraphic levels *D.*
321 *ovum* shells had bimodal or multimodal compass orientations with a prevailing north-
322 northeast to south-southwest flow axis (mean $197^o \pm 4^o$) throughout the upper half of
323 the *bifrons* Zone (Supplementary Information Fig. S1).

©2020, Elsevier. This manuscript version is made available under the CC-BY-NC-ND 4.0 license http://creativecommons.org/licenses/by-nc-nd/4.0/

3.2 Shell size and shape of *Dacryomya ovum*

Dacryomya ovum mean shell size fluctuated approximately two fold throughout its stratigraphic range, up to 10 mm shell length and 4.5 mm shell height (Fig. 4). Median shell length (Kruskal Wallis, $X^2 = 231.6$, $p<0.001$), height (Kruskal Wallis, $X^2 = 109.8$, $p<0.001$) and inflation (Kruskal Wallis, $X^2 = 288.7$, $p<0.001$) significantly differed between the 30 assemblages. The Jonckheere Terpstra test showed that median shell length ($z= 6.95$, $p <0.001$) and inflation ($z = 13.02$, $p<0.001$) increased with stratigraphic height in the section. Overall the body fossils (i.e. with shell) were on average 3 mm shorter, 1 mm narrower and 3 mm less inflated compared with the internal moulds (Mann-Whitney U-test, $p<0.005$): therefore the broad stratigraphic trend of increasing size through time, is slightly underestimated (Figs 3-4).The morphometric indices revealed differences in the degree of *D. ovum* shell flexure (SDI1, Kruskal-Wallis test, $X^2 = 44.12$, $p = 0.027$) and elongation of the posterior end (SDI3, Kruskal Wallis test, $X^2 = 75.29$, $p<0.001$) between assemblages. *D. ovum* shell posterior-anterior asymmetry (SDI2, Kruskal-Wallis Test, $X^2 = 36.13$, $p >0.05$) did not differ between stratigraphic levels (Fig. 4).

The morphometric data were subdivided into two groups based on TOC content (<2% or >2% wt.) and the median shell height, length, elongation and flexure were lower when TOC was >2% (Table 1). Thus, when TOC was high *D. ovum* shells were smaller and had greater posterior elongation and flexure.

Multiple regression showed that under conditions of low (<2%) sedimentary TOC mean shell length and width were positively correlated with TOC (Table 2). Higher TOC corresponded to larger shells presumably indicating a link with their food

©2020, Elsevier. This manuscript version is made available under the CC-BY-NC-ND 4.0 license http://creativecommons.org/licenses/by-nc-nd/4.0/

supply (organic matter). For maximum shell length the strongest predictor variable was TOC/TS a proxy for palaeoredox (Table 2) with high TOC/TS indicating greater oxygenation, corresponded to larger shells. Of the geochemical proxies only TOC and TOC/TS (Pearson's correlation r = 0.724, p = 0.004, n=30) were correlated with each (at p>0.01), but this may be due to their common derivation. However, model statistics did not indicate any multicolinearity in the regressions (Table 2). All but one stepwise multiple regression showed a significant influence of TOC (Table 2) and excluded TOC/TS. It seems therefore that primary productivity had a greater effect on shell size, and any direct effects of palaeoredox were not established.

When TOC exceeded 2% multiple regression with bivalve size (mean shell length, width or maximum length) was not significant ($p<0.05$) suggesting that either: bivalve size was only related to TOC when organic matter supply was low, and thus food supply was limited, or that conditions were more reducing when TOC was >2% and this confounded the influence of food supply on bivalve growth. *D. ovum* did not occur in facies with less than ~1% TOC (Fig. 4). There was no correlation between bivalve density and size that might indicate intraspecific competition for resources restricted growth.

D. ovum shell length was strongly positively correlated with shell height (reduced major axis regression on log-transformed data, $R^2 = 0.48$, $t = 27.89$, $p<0.001$; $a = 1.18$) and weakly correlated with shell inflation ($R^2 = 0.18$, $t = 11.670$ $p<0.001$, $a = 0.43$)(Supplementary Information Fig. S2). The relationship between shell height and inflation was significant but very weak ($R^2 = 0.03$, $t = 4.08$, $p<0.001$, $a = 2.28$). The relative rates of growth between age-dependent morphometric variables such as these can indicate whether proportionate or disproportionate

©2020, Elsevier. This manuscript version is made available under the CC-BY-NC-ND 4.0 license http://creativecommons.org/licenses/by-nc-nd/4.0/

(allometric) growth occurs between the different morphometrics. The allometric exponent (equivalent to the slope of the regression line when data are log-transformed) of the relationship between *D. ovum* shell height and shell length was >1 meaning that in *D. ovum* allometry between shell height and length was positive. Thus, *D. ovum* growth was disproportionate: with height increasing faster than length.

Shell growth patterns were examined for a small number of well-preserved body fossils to achieve an overview of *D. ovum* growth. In many cases external growth bands were prominent and numerous (e.g. Fig. 2C–E), and the most distinct (as indicated by their thickness, topography, texture and colour) were interpreted to be annuli. This interpretation of annuli is supported by the growth patterns for the *D. ovum* specimens (Fig. 5B) that fit the von Bertalanffy growth model (R^2 >0.99, $p<0.05$). Shells were aged between 7 and 9 years, and population growth rates (ω) ranged from 3.75 to 6.80.

3.3 Population structure

The length frequency distributions (LFDs) from each of the 30 assemblages showed that the *D. ovum* population dynamics varied through time (Fig. 3A). One third of the shell pavements had unimodal size distributions (the majority having a mode $\geq$16 mm), and the remainder were multimodal indicating that at most levels more than one size cohort was present. Fifteen LFDs were negatively skewed, five were approximately normal and ten were positively skewed (Fig. 3A). Both the shell length range and the number of modes increased throughout the species stratigraphic range: with most LFDs being positively skewed below 44 m (mean skew -0.06) and normal or negatively skewed above 44 m (mean skew 0.15). The LFDs of

©2020, Elsevier. This manuscript version is made available under the CC-BY-NC-ND 4.0 license http://creativecommons.org/licenses/by-nc-nd/4.0/

401 the bivalve species that dominated the seafloor at the onset (*tenuicostatum*
402 Subzone), during (*exaratum* Subzone) and after the Toarcian OAE (*falciferum*
403 Subzone) are very different from those for *D. ovum* (Fig. 3B).

404 There were no shells in length classes <8 mm in any *D. ovum* assemblage
405 (Fig. 3A), and there was no taphonomic evidence (e.g. sedimentary features
406 indicating currents or shell fragments) for size selective removal of these smaller
407 shells. However, differences in the preservation of body fossils throughout the
408 section (Table S1) suggest some diagenetic dissolution may have occurred.

409

410 **3.4 Benthic community change**

411 In the Cleveland Basin benthic communities of the upper *falciferum* and lower
412 *commune* subzones (between 26 m and 35 m) were dominated by the bivalve *M.*
413 *substriata* with occasional occurrences of *P. dubius*, *B. buchi*, the brachiopod *L.*
414 *longovicensis* and the gastropod *Ptychomphalus expansus* (Fig. 4; Little 1995, 1996).
415 TOC content was initially high and decreased to ~ 2% TOC between 38.01 m and
416 41.71 m; (Fig. 4), and *D. ovum* appeared at ~38.60 m (Fig. 4). Throughout its
417 sampled stratigraphic range *D. ovum* abundance varied 10 fold, reaching a maximum
418 at ~41.0 m, followed by a general decline through time (Fig. 4). The abundance of
419 the other bivalve species *B. buchi, M. substriata* and *G. donaciformis* (Fig. 4)
420 increased above 44 m but these taxa were less abundant than *D. ovum* that
421 dominated throughout the main Alum Shale.

422

423 Mean TOC decreased from 2.16% to 1.94% above 41.71 m (Fig. 4), and
424 pyritised trace fossils appeared at 42 m, their first occurrence since before the OAE.
425 The highest *D. ovum* abundances did not correspond with high trace fossil

©2020, Elsevier. This manuscript version is made available under the CC-BY-NC-ND 4.0 license http://creativecommons.org/licenses/by-nc-nd/4.0/

abundances (Fig. 4). Above 47–48 m trace fossil abundance markedly increased although remained variable.

4. Discussion

The present study explored changes within the early successional benthic communities present ~900 kyr after the end of the Toarcian OAE (based on the timescale of Kemp et al. 2011), as geochemically defined (Pearce et al. 2008), in the Cleveland Basin, Yorkshire, UK. At this time the Earth was recovering from a global warming event that was comparable with the changes predicted under the highest IPCC pCO_2 emissions scenario that predicts a 7.5^{o}C atmospheric temperature rise by 2100 (IPCC, 2103). The Cleveland Basin benthos remained species poor for >900 kyr after the OAE (Caswell and Frid 2017), and the recovering seafloor communities of the *bifrons* Zone consisted predominantly of near-monospecific occurrences of the bivalve *D. ovum*. Other bivalve species were occasionally abundant. Together with the geochemical proxy data (Pearce et al. 2008; Raiswell et al. 1983) this suggests that conditions remained deoxygenated at times. Thibault et al. (2018) concluded that at least the lower half of the *commune* Subzone was dysoxic. In the upper *commune* Subzone (~42 m) macroinfauna reappeared, as shown by the presence of trace fossils. The improving sedimentary conditions coincided with a shift from near-monospecific communities of *D. ovum* to a more diverse assemblage (Fig. 4; Danise et al. 2013; Little 1996) with a greater range of life and feeding habits (Caswell and Frid 2017).

Nuculanid Jurassic deposit feeders such as *Dacryomya* and *Nuculana* spp. were geographically widely distributed during the Pliensbachian and Toarcian Stages. Both taxa predominantly occurred in mudstones and marlstones (Supporting Information Table S2), indicating a preference for organic-rich substrates. These

©2020, Elsevier. This manuscript version is made available under the CC-BY-NC-ND 4.0 license http://creativecommons.org/licenses/by-nc-nd/4.0/

453 occurrences suggest that *Dacryomya* was tolerant of low oxygen conditions (Marinov
454 et al. 2006) similar to *Nuculana* species today (Holmes et al. 2002). *Dacryomya* spp.
455 Seem to have been 'enrichment opportunists' meaning that they were the initial
456 colonizers in organic rich formerly anoxic areas (and so differ somewhat from general
457 opportunists; Pearson and Rosenberg 1978). The occurrences of the first infaunal
458 taxon, *D. ovum,* after the OAE are important because burrowing animals would have
459 mixed and reoxygenated the sediments increasing the habitat available to less
460 tolerant taxa. Thus, the establishment of burrowers, such as *D. ovum,* would have
461 facilitated the recovery of the Toarcian benthos.

462

463 Very few broken or disarticulated shells occurred in the shell pavements
464 suggesting generally low energy conditions and minimal post-mortem disturbance.
465 The *D. ovum* pavements are therefore autochthonous or parautochthonous. Watson
466 (1982) suggested that, in the upper *commune* Subzone, *D. ovum* infilled with mud
467 matrix and oriented orthogonal to the bedding were better preserved. The data from
468 this study supports this suggestion: above 47 m shell compaction decreased, and a
469 higher proportion were preserved as internal moulds. This variable preservation of
470 the aragonite shells could be due to variations in the vertical position of the redox
471 boundary: when the boundary was at the surface the material below was less likely
472 to dissolve because it was below the taphonomically active zone (Cherns et al. 2008;
473 Wright et al. 2003). The lack of body fossils, and the predominance of internal
474 moulds, above 47 m could therefore indicate changes in the vertical position of the
475 redox boundary in the *fibulatum* Subzone. Further high resolution geochemical proxy
476 data are needed to confirm these changes.

477

©2020, Elsevier. This manuscript version is made available under the CC-BY-NC-ND 4.0 license http://creativecommons.org/licenses/by-nc-nd/4.0/

4.1 Palaeoecology

During deoxygenation extant burrowing animals migrate towards the sediment surface to facilitate access to oxygen, and when low oxygen conditions persist they leave their burrows entirely and live on the surface until conditions improve (e.g. Baden et al. 1990; Long et al. 2014; Norrko and Bonsdorff 1996; Rosenberg and Loo 1988). As conditions deteriorate further they extend their appendages or entire body up into the water column to access the oxygenated water (Nilsson and Rosenberg 1994; Reidel et al. 2014; Rosenberg et al. 1991). For instance, many bivalve species have been observed to extend their siphons up into the water column during deoxygenation (Rosenberg and Loo 1988; Taylor and Egglestone 2000, Seitz et al. 2003; Tallqvist 2001). We hypothesise that *D. ovum* also behaved in this way during deoxygenation.

The morphology of *D. ovum* suggests that the usual life position would have been at shallow sediment depths with the long-axis oriented approximately vertically and the rostrate posterior and siphons projected towards the sediment surface (Stanley 1970; Stanley 1981). Observations of the brachiopod *Discinisca infraoolitica* preferentially attached to the posterior end of *D. ovum* in the upper *commune* Subzone (Watson 1982) support such a living habit. The suspension feeding epibionts all had their anterior, feeding, end oriented towards the posterior of *D. ovum* where they would have benefitted from the inhalent and exhalent currents (Watson 1982), thus the posterior ends *D. ovum* would have been habitually emerged above the sediment surface during life. *D. ovum* shells were often oriented concordant to the bedding (i. e. not in life position) and, because there was minimal evidence for post-mortem disturbance, these occurrences suggest that *D. ovum* may have adopted an epifaunal life habit at times (i.e. during bottom water anoxia).

©2020, Elsevier. This manuscript version is made available under the CC-BY-NC-ND 4.0 license http://creativecommons.org/licenses/by-nc-nd/4.0/

505 The present study showed that, although some aspects of *D. ovum* shell
506 shape were similar between assemblages, there were variations in the extent of
507 posterior-anterior asymmetry and elongation of the posterior end of the shell. Such
508 shape changes would have been advantageous for reaching oxygenated parts of the
509 water column during deoxygenation. For instance, in present-day hypoxic sediments
510 *M. balthica* shells have more elongated posterior ends an adaptation that facilitates
511 siphon extension into oxygenated water (Sokolowski et al. 2008). The posterior
512 elongation of *D. ovum* in Yorkshire might also have been an adaptation to
513 deoxygenation (Fig. 2B–H).

514

515 ### *4.2* Shell size and growth

516 The *D. ovum* shells from the Cleveland Basin were up to six times larger than
517 Sinemurian *Dacryomya heberti* and 3–4 times larger than Pliensbachian and
518 Oxfordian *Dacryomya* spp. (Delvene 2000; Hodges 2000; Table 3). The mean length
519 of *D. ovum* varied by up to 8 mm throughout its stratigraphic range in Yorkshire,
520 although this is probably an underestimate of up to 3 mm due to the lack of a shell for
521 most specimens (the internal moulds) in the *fibulatum* Subzone (Fig. 4). The
522 variations in *D. ovum* size, and thus growth, could be due to density dependent
523 factors (Olafsson 1986), changes in food supply (Beukema and Cadée 1991;
524 Carmichael et al. 2004; Kirby and Miller 2005; Schöne et al. 2005; Thompson and
525 Nichols 1988), temperature, salinity (e.g., Ambrose Jr. et al. 2006; Johnson 1999;
526 Schöne et al. 2005) or deoxygenation (Long et al. 2014). *D. ovum* body size was
527 correlated with TOC when TOC was <2%, and conditions were presumably more
528 oxygenated, which is supported by a higher abundance of trace fossils (Fig. 4). The
529 absence of statistical relationships between shell size and shell density, proxies for
530 surface seawater temperature ($\delta^{18}O_{bel}$) and independent proxies for palaeoredox
531 ([Mo], [U], Th/U, U/Th, DOP) suggest a link with organic matter and so food supply.

©2020, Elsevier. This manuscript version is made available under the CC-BY-NC-ND 4.0 license http://creativecommons.org/licenses/by-nc-nd/4.0/

532 Surface deposit feeders such as *Dacryomya* could have directly fed on labile surface
533 organic matter or the sedimentary microbes that process it (Lopez and Levinton
534 1987; Levinton and Bianchi 1981). They are unlikely to have efficiently consumed the
535 legacy organic matter that accumulates at depth within the sediments (Levinton and
536 Kelaher 2003; Mayer et al. 1997). So like the suspension feeding opportunists during
537 the OAE (Caswell and Coe 2013) the *Dacryomya* may also be responding to
538 variations in fluxes of organic matter from primary production in the photic zone.

539

540 The main influences on the TOC content of sedimentary rocks are primary
541 production and organic matter preservation (Arthur and Sageman 1994), and the
542 latter is primarily controlled by sedimentation rate not bottom water oxygen levels
543 (Betts and Holland 1991). The lack of a timescale for the *bifrons* zone in Yorkshire
544 means the influence of variations in sedimentation rate on TOC cannot be excluded,
545 but cyclostratigraphic data from the *falciferum* and *tenuicostatum* zones suggest that
546 sedimentation rates did not vary much (Kemp et al. 2011). The range of TOC
547 concentrations recorded in the *bifrons* Zone are similar to the lower end of the
548 sedimentary TOC ranges found in comparable present-day deoxygenated areas (e.g.
549 1.5–6.5% TOC in continental margin sediments, and 3-15% TOC in anoxic silled
550 basin sediments; Demaison and Moore 1980; Levin and Gage 1998). Similar to
551 *Dacryomya*, present-day seafloor communities show relationships between
552 macrofaunal body-size and TOC: under intermediate levels of deoxygenation, taxa
553 that are tolerant of deoxygenation show increased body size due to organic
554 enrichment (e. g., Borja et al. 2000; Caswell and Frid 2018; Fuksi et al. 2018; Weston
555 1990). For instance, changes in the size of the bivalve *Corbula gibba* in
556 deoxygenated and oxygenated areas of the Adriatic Sea over the last c. 10 ka were
557 due to changes in TOC content (Fuksi et al. 2018) that are of a similar magnitude to
558 those found in the present-study.

©2020, Elsevier. This manuscript version is made available under the CC-BY-NC-ND 4.0 license http://creativecommons.org/licenses/by-nc-nd/4.0/

559

560 During the OAE the body size of the dominant species, *P. dubius*, in
561 Yorkshire decreased by up to 50%, and these changes were also linked with primary
562 productivity (Caswell and Coe 2013). In the French and Spanish early Toarcian
563 sections 11 bivalve species that occur in abundance after the OAE (*commune* and
564 *fibulatum* zones) had maximum body sizes 26–82% smaller than their other Jurassic
565 occurrences (Fürsich et al. 2001). These small sizes were interpreted to reflect
566 stunted growth due to an inadequate food supply (Fürsich et al. 2001). Overall, it
567 seems that considerable changes in body size occurred both during and for some
568 time after the Toarcian OAE in the Cleveland Basin, Yorkshire, and in the mid to
569 lower shelf environments in Spain and France, respectively and that these changes
570 were predominantly driven by changes in primary productivity and thus food supply.
571 On the margins of the Panthalassa Ocean, at sections exposed in Alberta, Canada,
572 both bivalves and brachiopods exhibited body-size reductions during the OAE and
573 remained small in the aftermath (during the *planulata* Zone which is equivalent to the
574 *bifrons* zone)(Martindale and Aberhan 2017).

575

576 Major changes in the phytoplankton assemblage composition and microfossil
577 body-size during and immediately after the Toarcian OAE (*falciferum* Zone;
578 Clemence et al. 2015; Martindale and Aberhan 2017; Mattioli et al. 2008; Palliani et
579 al. 2002; Vania et al. 2017) support the suggestion that at times food limitation
580 restricted bivalve body-size. Collapses in primary productivity have occurred during
581 other mass extinctions including the Late Devonian (Girard and Renaud 1996),
582 Permian–Triassic (Twitchett 2006), Triassic/Jurassic boundary (Ward et al. 2004)
583 and Cretaceous/Tertiary boundary (Smith and Jeffery 1998). Notable body-size

©2020, Elsevier. This manuscript version is made available under the CC-BY-NC-ND 4.0 license http://creativecommons.org/licenses/by-nc-nd/4.0/

584 decreases followed three of these events and conform to what is known as the
585 'Lilliput effect' (Urbanek 1993).

586

587 **4.3 Population dynamics**

588 In low energy environments such as those of the *bifrons* Zone, where
589 taphonomic processes are reduced, the LFDs of brachiopod death assemblages
590 have been shown to have high fidelity with the life assemblages (Tomasovych 2004),
591 and so the skew and modality of the LFDs can be used to reliably infer population
592 structure. The length frequency distributions (LFDs) of *D. ovum* were mostly
593 indicative of mature populations with multiple size cohorts (Fig. 3B), and through time
594 as the environmental conditions improved they became more skewed towards the
595 larger size classes. Changes in the mean and maximum shell length also reflect this
596 shift. However, the absence of *D. ovum* shells <8 mm across all assemblages, and
597 the lack of any signs of physical disturbance, could suggest post mortem dissolution
598 of the smallest shells (Dodd and Stanton Jr. 1990). However, Tomasovych (2004)
599 showed that even when shell dissolution occurs it is incomplete and significant
600 numbers of juvenile shells often remain. The complete absence of juveniles *D. ovum*
601 therefore suggests it had low recruitment and/or juvenile mortality.

602

603 The LFDs of the dominant bivalves during the OAE in Yorkshire (Fig. 3B),
604 France and Germany although different from the LFDs for *D. ovum* all showed a
605 similar trend to that observed in this study. In Yorkshire *B. radiata* and *P. dubius*
606 LFDs were strongly positively skewed during the OAE and the strength of the skew
607 weakened as conditions improved (Caswell and Coe 2013). In SW Germany *B.*
608 *buchi, P. dubius* and *M. substriata* (Röhl 1998; Röhl et al. 2001) and in southern
609 France *Dacryomya lacrymya* (Fürsich et al. 2001) LFDs also shifted from positively

©2020, Elsevier. This manuscript version is made available under the CC-BY-NC-ND 4.0 license http://creativecommons.org/licenses/by-nc-nd/4.0/

skewed unimodal through to normal and/or negatively skewed multimodal LFDs after the OAE. In Alberta although this general pattern was followed there were distinct differences between taxa. *Meleagrinella* and *Bositra* exhibited strongly positively skewed LFDs *Pseudomytiloides* did not, and in strata coeval with the *bifrons* Zone in NW Europe recovery is not apparent for *Meleagrinella* (Martindale and Aberhan 2017).

In present-day deoxygenated areas populations of tolerant bivalves have life assemblages dominated by juveniles, with LFDs that are positively skewed reflecting strong recruitment but low survival into adulthood (Long et al. 2014; Powers et al. 2005). Death assemblages from present-day deoxygenated areas may also produce strongly positively skewed LFDs reflecting high juvenile mortality (Fig. 2B). Opportunist taxa with very high fecundity, fast growth and generation times may take advantage of the brief periods of oxygenation and establish large populations very rapidly (Caswell and Coe 2013). Other tolerant bivalves for example *M. balthica* may be able to continue to reproduce during low oxygen conditions, e.g. at <2 mgl^{-1} dissolved oxygen *M. balthica* continues to reproduce although fecundity decreases by ~75%; and, at <1.5 mgl^{-1} *M. balthica* recruit but do not attain reproductive age (Long et al. 2014). Long et al. (2014) showed that present-day populations of *M. balthica* may be supported by recruitment from nearby oxygenated areas, up to some threshold beyond which the increases in the extent and duration of hypoxia results in local extinction.

The number of growth lines on *D.ovum* shells of 20 mm shell height ranged between seven and nine (Fig. 5) suggesting that, if these were annuli, *D. ovum* lived for up to 9 years which is within the range for present-day species of this family across northern temperate latitudes (Moss et al. 2017; Nakaoka and Matsui, 1994). The population structure and growth curves (Fig. 5) together suggest that *D. ovum* had the attributes of a K-strategist (i.e. one with a relatively long lifespan and low

©2020, Elsevier. This manuscript version is made available under the CC-BY-NC-ND 4.0 license http://creativecommons.org/licenses/by-nc-nd/4.0/

reproductive output; MacArthur 1960). Similarly, older *Dacryomya* spp. from the Sinemurian and Pliensbachian of the southwest UK have LFDs that are indicative of populations with more mature individuals (Hodges 2000). Contrastingly, *P. dubius,* which dominated during the OAE, seems to have had an opportunistic life history and may have reproduced after just a few months (Caswell and Coe 2013).

4.4 Changes in seafloor communities

The Toarcian OAE was associated with a mass extinction of benthic and pelagic marine invertebrates across the Boreal and Tethyan realms (Aberhan 2002; Caswell et al. 2009; Cecca and Macchioni 2004; Little and Benton 1995; Ruban 2004; Voros 2002; Zakharov 2006). Across NW Europe the seafloor macrofaunal palaeocommunities were of very similar composition during the OAE being dominated by 2–3 bivalve species only throughout the *falciferum* Zone in the Cleveland Basin, UK, Paris Basin and SW German basins (Caswell et al. 2009; Fürsich et al. 2001; Riegraf 1982; Röhl 1998; Röhl et al. 2001). Furthermore, the benthic assemblages on the margins of the Panthalassa Ocean were also remarkably similar to NW Europe (Martindale and Aberhan 2017). Taxa at higher trophic levels were also affected e.g. marine reptiles and cephalopods in NW Europe (Caswell and Coe 2014; Maxwell and Vincent 2016). Subsequently, an impoverished benthos persisted across NW Europe, and as conditions improved (*commune* and *fibulatum* subzones; Fig. 4), benthic communities became dominated by species, with affinities for organic rich substrates, and a greater diversity of life and feeding habits (e.g., Caswell and Frid 2017; Danise et al. 2013; Fürsich et al. 2001; Röhl 1998). In Yorkshire the trace fossils were predominantly those of shallow burrowers with morphologies of grazers or deposit feeders (Martin 2004, Sellwood 1972).

©2020, Elsevier. This manuscript version is made available under the CC-BY-NC-ND 4.0 license http://creativecommons.org/licenses/by-nc-nd/4.0/

Three ecologically significant changes are apparent, from both the body and trace fossil data from the Alum Shale of the Cleveland Basin (Fig. 4). **(1)** In the mid *commune* Subzone *D. ovum* abundance increased sharply and these populations became established. **(2)** In the upper *commune* Subzone, at 42 m, trace fossils re-appeared, having been absent since before the start of the OAE, and body fossils of the deep burrower *Gresslya donaciformis* occurred (Fig. 4). **(3)** The degree of bioturbation markedly increased at the base of the *fibulatum* Subzone and, although variable, increased throughout the subzone. These changes show stepped improvements in conditions on the seafloor that indicate increasing oxygenation. This interpretation is consistent with the stepped decreases in TOC and a suite of other geochemical proxies that show that although conditions were generally deoxygenated in the *bifrons* Zone, oxygenation was increasing (including TS/TOC, Degree of Pyritisation of Fe, [Mo], Re/Mo and $\partial^{98/95}$Mo; Pearce et al. 2008; Raiswell et al. 1993; Thibault et al. 2018).

The temporal variations in trace fossil abundance, *D. ovum* abundance and preservation likely reflect fluctuations in the degree of oxygenation and vertical position of the redox boundary throughout much of the *commune* Subzone. Deoxygenation probably varied seasonally or episodically throughout the OAE with reoxygenation becoming more prolonged throughout the *bifrons* Zone leading to higher benthic diversity (Caswell and Frid 2017, Levin and Gage 1998). A present-day study of bioturbation along an oxygenation gradient in the Oman Margin Oxygen Minimum Zone showed that below 0.13–0.27 ml l^{-1} dissolved oxygen burrowing was substantially reduced (Demaison and Moore 1980; Smith et al. 2000). Furthermore, benthic scavengers were absent below 0.3–0.5 ml l^{-1} dissolved oxygen (Demaison and Moore 1980). The apparent absence, or low abundance of, both scavengers and

©2020, Elsevier. This manuscript version is made available under the CC-BY-NC-ND 4.0 license http://creativecommons.org/licenses/by-nc-nd/4.0/

689 bioturbators in the Cleveland Basin suggests that at times dissolved oxygen levels
690 were below 0.5 ml l^{-1}.

691

692 The lack of correspondence between high *D. ovum* abundance and increased
693 bioturbation suggests that even though *D. ovum* had an infaunal life habit it was not
694 living infaunally below 42 m stratigraphic height (Fig. 4). The appearance of trace
695 fossils and the increased abundance of other taxa only after *D. ovum* became
696 established suggests it may have performed an ecosystem engineering role enabling
697 other taxa to become resident. Further investigation of the associations between
698 body and trace fossils could help to better understand the benthic successional
699 changes during recovery from the OAE.

700 ## 5. Conclusions

701 *Dacyomya ovum* like other members of the genus had a preference for
702 organic rich substrates, and after the Toarcian OAE it was the first infaunal taxon to
703 occur in abundance and so was an important pioneer species. The population
704 structure, size and growth data suggest *D. ovum* was a K-strategist, and at
705 intermediate levels of deoxygenation for *Dacryomya*, like tolerant taxa today, body
706 size was linked with organic enrichment. Variations in the body size and population
707 structure of bivalves were evident both during and after the early Toarcian event from
708 contemporaneous sections in the UK, France, Spain, Germany and Canada; and,
709 are similar to those observed for present-day bivalves exposed to deoxygenation. In
710 NW Europe the body size changes were attributable to changes in the food supply of
711 the dominant benthic taxa, and show that changes in primary productivity had a
712 major influence on benthic ecosystems both during and after the OAE.

713 After the Toarcian OAE an impoverished benthos persisted across NW
714 Europe, and as conditions slowly improved in the *commune* and *fibulatum* subzones
715 diversity increased and benthic communities became dominated by species, with

©2020, Elsevier. This manuscript version is made available under the CC-BY-NC-ND 4.0 license http://creativecommons.org/licenses/by-nc-nd/4.0/

affinities for organic rich substrates, and infauna became re-established. The absence, or low abundance of, trace fossils in the lower *bifrons* Zone in Yorkshire suggest that dissolved oxygen was below 0.5 ml l^{-1} at times. Infauna can perform important ecosystem engineering roles and make substantial contributions to benthic ecosystem functioning. Improved understanding of the successional changes within the infaunal communities after the OAE are important for understanding the consequences of deoxygenation and the recovery processes in present-day marine ecosystems threatened by anthropogenic climate change.

Acknowledgments

Thanks to Alice Kennedy, Paul Scott and Joseph McCarten for assistance in the field. This work benefitted from constructive discussions with Chris Frid, Angela Coe, and Liam Herringshaw. The work was partially supported by a project stipend to SD from the University of Liverpool. Infrastructure and facilities provided by the Universities of Liverpool, University of Hull, UK and the Environmental Futures Research Institute, Queensland.

©2020, Elsevier. This manuscript version is made available under the CC-BY-NC-ND 4.0 license http://creativecommons.org/licenses/by-nc-nd/4.0/

References

Aberhan, M., 1998. Paleobiogeographic patterns of pectinoid bivalves and the Early Jurassic tectonic evolution of Western Canadian Terranes. Palaios 13,129–148.

Aberhan, M., 2002. Opening of the Hispanic Corridor and Early Jurassic bivalve biodiversity. Geological Society Special Publication 194,127–139.

Al-Suwaidi, A.H., Angelozzi, G.N. Buadin, F., Damborenea, S.E., Hesselbo, S.P., Jenkyns, H.C., Mancenido, M.O., Riccardi, A.C., 2010. First record of the Early Toarcian Oceanic Anoxic Event from the Southern Hemisphere, Neuquén Basin, Argentina. J. Geol. Soc., London 167, 633–636.

Ambrose Jr., W.G., Carroll, M.L., Greenacre, M.J., Thorrold, S.R., McMahon, K.W., 2006. Variation in *Serripes groenlandicus* (Bivalvia) growth in a Norwegian high-Arctic fjord: evidence for local- and large-scale climatic forcing. Glob. Change Biol. 12, 1595–1607.

Arthur, M. A., Sageman, B. B. 1994. Marine black shales: depositional mechanisms and environments of ancient deposits. Annu. Rev. Earth Planet. Sci. 22, 499–551.Baden, S.P., Loo, L.O., Pihl, L., Rosenberg, R., 1990. Effects of eutrophication on benthic communities including fish: Swedish west coast. Ambio 19, 113–122.

Bailey, T.R., Y. Rosenthal, J.M. McArthur, B. van de Schootbrugge, Thirlwall, M.F., 2003. Paleoceanographic changes of the Late Pliensbachian-Early Toarcian interval: a possible link to the genesis of an Oceanic Anoxic Event. Earth Planet. Sc. Lett. 212, 307–320.

Betts, J.N., Holland, H.D. 1991. The oxygen content of ocean bottom waters, the burial efficiency of organic carbon, and the regulation of atmospheric oxygen. Palaeogeogr. Palaeoecol. 97, 5–18.

Beukema, J.J., Cadée, G.C., 1991. Growth rates of the bivalve *Macoma balthica* in the Wadden Sea during a period of eutrophication: relationships with concentrations of pelagic diatoms and flagellates. Mar. Ecol-Prog. Ser. 68, 249–256.

Breitburg, D., Levin, L.A., Oschlies, A., Grégoire, M., Chavez, F.P., Conley, D.J., Garçon, V., Gilbert, D., Gutiérrez, D., Isensee, K., Jacinto, G.S., Limburg, K.E., Montes, I., Naqvi, S.W.A., Pitcher, G.C., Rabalais, N.N., Roman, M.R., Rose, K.A., Seibel, B.A., Telszewski, M., Yasuhara, M., Zhang, J., 2018. Declining oxygen in the global ocean and coastal waters. Science 359, 1–13.

Borja, A., Franco, J., Perez, V., 2000. A marine biotic index to establish the ecological quality of soft-bottom benthos within European estuarine and coastal environments. Mar. Poll. Bull. 40, 1100–1114.

Carmichael, R.H., Shriver, A.C., Valiela, I., 2004. Changes in shell and soft tissue growth, tissue, composition, and survival of quahogs, *Mercenaria mercenaria*, and softshell clams, *Mya arenaria*, in response to eutophic-driven changes in food supply and habitat. J. Exp. Mar. Biol. Ecol. 313, 75–104.

Carroll, M.L., Ambrose Jr., W.G., Levin, B.S., Ryan, S.K., Ratner, A.R., Henkes, G.A., Greenacre, M.J., 2011. Climatic regulation of *Clinocardium ciliatum* (Bivalvia) growth in the northwestern Barents Sea. Palaeogeogr. Palaeoecol. 302, 10–20.

Caruthers, A.H., Gröcke, D.R., Smith, P.L., 2011. The significance of an Early Jurassic (Toarcian) carbon-isotope excursion in Haida Gwaii (Queen Charlotte Islands), British Columbia, Canada. Earth Planet. Sc. Lett. 307, 19–26.

Caswell, B.A., Coe, A. L., 2013. Primary productivity controls on opportunitsic bivalves during Early Jurassic oceanic anoxia. Geology 41, 1163–1166.

Caswell, B.A., Coe, and A.L., 2014. The impact of anoxia on pelagic macrofauna during the Toarcian Oceanic Anoxic Event (Early Jurassic). P. Geologist. Assoc. 125, 383–391.

Caswell, B.A., Coe, A.L. Cohen, A.S., 2009. New range data for marine invertebrate species across the early Toarcian (Early Jurassic) mass extinction. J. Geol. Soc., London 166, 859–872.

Caswell, B.A., Frid, C.L.J., 2017. Marine ecosystem resilience during extreme deoxygenation: the Early Jurassic oceanic anoxic event. Oecologia 183, 275–290.

Cecca, F., Macchioni, F. 2004. The two Early Toarcian (Early Jurassic) extinction events in ammonoids. Lethaia 37, 35-56.

Cherns, L., Wheeley, J.R., Wright, V.P., 2008. Taphonomic windows and molluscan preservation. Palaeogeogr. Palaeoecol. 270, 220–229.

©2020, Elsevier. This manuscript version is made available under the CC-BY-NC-ND 4.0 license http://creativecommons.org/licenses/by-nc-nd/4.0/

792 Cheung, W.L., Sarmiento, J.L., Dunne, J., Frolicher, T.L., Lam, V.W.Y., Deng Palomares,
793 M.L., Watson, R., Pauly, D., 2013. Shrinking of fishes exacerbates impacts of global
794 ocean changes on marine ecosystems. Nature Climate Change 3, 254–258.
795 Clemence, M.-E., Gardin, S., Bartolini, A., 2015. New insights in the pattern and timing of the
796 Early Jurassic calcareous nannofossil crisis. Palaeogeogr. Palaeoecol. 427,100–108.
797 Cohen, A.S., Coe, A.L., Harding, S.M., Schwark, L., 2004. Osmium isotope evidence for the
798 regulation of atmospheric CO_2 by continental weathering. Geology 32, 157–160.
799 Damborenea, S.E., 1987. Early Jurassic bivalvia of Argentina. Part 2: Superfamilies
800 Pteriacea, Buchiacea and part of Pectinacea. Palaeontographica Abt. A 199:113–
801 216.
802 Danise, S., Twitchett, R.J., Little, C.T.S., Clemence, M.-E., 2013. The Impact of Global
803 Warming and Anoxia on Marine Benthic Community Dynamics: an Example from the
804 Toarcian (Early Jurassic). Plos One 8:1–14.
805 Danise, S., Twitchett, R. J., Little, C. T. S., 2015. Environmental controls on Jurassic marine
806 ecosystems during global warming. Geology 43, 263–266.
807 Delvene, G., 2000. Taxonomie und Palökologie der Bivalven im Mittel- und Oberjura der
808 Keltiberischen Ketten (Spanien). PhD Thesis, Universität Würzburg, Würzburg, pp.
809 199.
810 Demaison, G.J., Moore, G.T., 1980. Anoxic environments and oil source bed genesis. Org.
811 Geochem. 2, 9–31.
812 Dera, G., Niege, P., Dommergues, J.-L., Brayard, A., 2011. Ammonite palaeobiogeography
813 during the Pliensbachian –Toarcian crisis (Early Jurassic) reflecting the
814 palaeoclimate, eustasy, and extinctions. Global Planet. Change 78, 92–105.
815 Diaz, R.J., Rosenberg, R., 2008. Spreading dead zones and consequences for marine
816 ecosystems. Science 321, 926–929.
817 Dodd, R.J., Stanton Jr., R.J., 1990. Paleoecology concepts and applications. John Wiley and
818 Sons, New York.
819 Emerson, C.W., Minchinton, T.E., Grant, J. 1988. Population structure, biomass, and
820 respiration of *Mya arenaria* L. on temperate sandflats. J. Exp. Mar. Biol. Ecol. 115,
821 99–111.
822 Falkowski, P.G., Hopkins, T.S., Walsh, J.J., 1980. An analysis of factors affecting oxygen
823 depletion in the New York Bight. J. Mar. Res. 38, 479–506.
824 Fuksi, T., Tomasovych, A., Gallmetzer, I., Haselmair, A., Zuschin, M., 2018. 20th centruy
825 increase in body size of a hypoxia-tolerant bivalve documented by sediment cores
826 from the northern Adriatic Sea (Gulf of Trieste). Mar. Poll. Bull. 135, 361–375.
827 Fürsich, F.T., Berndt, R., Scheuer, T., Gahr, M., 2001. Comparative ecological analysis of
828 Toarcian (Lower Jurassic) benthic faunas from southern France and east-central
829 Spain. Lethaia 34, 169–199.
830 Gahr, M.E., 2002. Palökologie des Makrobenthos im Unter-Toarc SW-Europas. Beringeria
831 31, 3–204.
832 Girard, C., Renaud, S., 1996. Size variation in conodonts in response to the Upper
833 Kellwasser crisis (Upper Devonian of the Montagne Noire, France). Cr. Acad. Sci. IIA
834 323, 435–442.
835 Gobbett, D.J. 1973. Permian Fusulinacea. Pp. 152–158 *in A.* Hallam, ed. Atlas of
836 palaeobiogeography. Elsevier, Amsterdam.Gomez, J.J., Arias, C., 2010. Rapid
837 warming and ostracods mass extinction at the Lower Toarcian (Jurassic) of central
838 Spain. Mar. Micropaleontol. 74, 119–135.
839 Graf, G., Rosenberg, R., 1997. Bioresuspension and biodeposition: A review. J. Marine Syst.
840 11, 269–278.
841 Gray, J.S., Wu, R.S.S., Or, Y.Y., 2002. Effects of hypoxia and organic enrichment on the
842 coastal marine ecosystem. Mar. Ecol-Prog. Ser. 238, 249–279.
843 Gröcke, D., Hori, R.S., Trabucho-Alexandre, J., Kemp, D.B., 2011. An open ocean record of
844 the Toarcian oceanic anoxic event. Solid Earth 2, 247–257.
845 Gutierrez, J.L., Jones, C.G., Strayer, D.L., Iribarne, O.O., 2003. Mollusks as ecosystem
846 engineers: the role of shell production in aquatic habitats. Oikos 101, 79-90.
847 Hammer, Ø., Harper, D.A.T., Ryan, P.D., 2001. PAST: Palaeontological Statistics Software
848 package for education and data anlysis. Palaeontologica Electronica 4, 1–9.
849 Hammer, Ø., Harper, D.A.T., 2006. Palaeontologcial data analysis. Blackwell Publishing,
850 Oxford.

©2020, Elsevier. This manuscript version is made available under the CC-BY-NC-ND 4.0 license http://creativecommons.org/licenses/by-nc-nd/4.0/

Harding, S.M., 2004. The Toarcian oceanic anoxic event: organic and inorganic geochemical anomalies in organic-carbon-rich mudrocks from the North Yorkshire Coast, UK and Dotternhausen Quarry, SW Germany. PhD thesis, The Open University, Milton Keynes, UK, 390 pp.

Håkansson, E., Thomsen, E. 1999. Benthic extinction and recovery patterns at the K/T boundary in shallow water carbonates, Denmark. Palaeogeogr. Palaeoecol. 154, 67–85.

Harries, P.J. 1993. Dynamics of survival following the Cenomanian–Turonian mass extinction event. Cretaceous Research 15, 563–583.

Haq, B., 2017. Jurassic sea level variations: A reappraisal. GSA Today 28, 4–10.

Hermoso, M., Le Callonnec, L., Minoletti, F., Renard, M., Hesselbo, S.P., 2009a. Expression of the Early Toarcian negative carbon-isotope excursion in separated carbonate microfractions (Jurassic, Paris Basin). Earth Planet. Sc. Lett. 277, 194–203.

Hermoso, M., Minoletti, F., Le Callonnec, L., Jenkyns, H. C., Hesselbo, S. P., Rickaby, R. E. M., Renard, M., de Rafélis, M., Emmanuel, L. 2009b. Global and local forcing of Early Toarcian seawater chemistry: A comparative study of different paleoceanographic settings (Paris and Lusitanian basins). Paleooceanography 24, 1-15.

Hesselbo, S.P., Gröcke, D.R. Jenkyns, H.C. Bjerrum, C.J. Farrimond, P. Morgans Bell, H.S., Green, O.R., 2000. Massive dissociation of gas hydrate during a Jurassic oceanic anoxic event. Nature 406, 392–395.

Hesselbo, S.P., Jenkyns, H.C., 1995. A comparison of the Hettangian to Bajocian successions of Dorset and Yorkshire. Pp. 105–150 *in* P. D. Taylor, ed. Field Geology of the British Jurassic. Geological Society, London.

Hesselbo, S.P., Jenkyns, H.C., 1998. British Lower Jurassic sequence stratigraphy. Pp. 561–581 *in* P. C. de Graciansky, J. Hardenbol, T. Jacquin, M. Farley, and P. R. Vail, eds. Mesozoic–Cenozoic Sequence Stratigraphy of European Basins. Special Publication of the Society for Sedimentary Geology, Society for Sedimentary Geology, Tulsa, USA.

Hesselbo, S.P., Jenkyns, H.C., Duarte, L.V., Oliveira, L.C.V., 2007. Carbon-isotope record of the Early Jurassic (Toarcian) Oceanic Anoxic Event from fossil wood and marine carbonate (Luisitanian Basin, Portugal). Earth Planet. Sc. Lett. 253, 455–470.

Hesselbo, S.P., Pienkowski, G., 2011. Stepwise atmospheric carbon-isotope excurison during the Toarcian Oceanic Anoxic Event (Early Jurassic, Polish Basin). Earth Planet. Sc. Lett. 301, 365–372.

Hodges, P., 2000. The Early Jurassic Bivalvia from the Hettangian and lower Sinemurian of south-west Britain. The Palaeontographical Society, London.

Holmes, S.P., Miller, N., Weber, A., 2002. The respiration and hypoxic tolerance of *Nucula nitidosa* and *N. nucleus*: factors responsible for determining their distribution? J. Mar. Biol. Assoc. UK 82, 971–981.

Horton, A., Edmonds, E.A., 1987. Geology of the country around Chipping Norton: memoir for 1: 50,000 geological sheet 218, new series (England and Wales) British Geological Survey.

Howarth, M.K., 1955. Domerian of the Yorkshire Coast. P. Yorks. Geol. Soc. 30, 147–175.

Howarth, M.K., 1962. The Jet Rock Series and the Alum Shale Series of the Yorkshire coast. P. Yorks. Geol. Soc. 33: 381–422.

Howarth, M.K., 1973. The stratigraphy and ammonite fauna of the upper 31iassic grey shales of the Yorkshire coast. Bull. Br. Mus. Nat. Hist. Geol. 24, 238–277.

Howarth, M.K., 1992. The Ammonite family Hildoceratidae in the Lower Jurassic of Britain. Monograph 586. The Palaeontographical Society, London.

IPCC. 2013. Climate Change 2013: the Physical Science Basis. UK and New York.

Jenkyns, H.C., 1988. The early Toarcian (Jurassic) anoxic event: Stratigraphic, Sedimentary, and Geochemical evidence. Am. J. Sci. 288: 101–151.

Jenkyns, H.C., 2010. Geochemistry of oceanic anoxic events. Geochem. Geophys. 11, 1–30.

Johnson, A.L.A., 1999. Evidence and cause of small size in Bathonian (Middle Jurassic) marine bivalves of North-Western Europe. Palaeontology 42, 605–624.

Jones, C.G., Lawton, J.H., Schachak, M., 1994. Organisms as ecosystem engineers. Oikos 69, 373–386.

Jones, D.S., Arthur, M.A., Allard, D.J., 1989. Sclerochronological records of temperature and growth from shells of *Mercenaria mercenaria* from Narragansett Bay, Rhode Island. Mar. Biol. 102, 225-234.

©2020, Elsevier. This manuscript version is made available under the CC-BY-NC-ND 4.0 license http://creativecommons.org/licenses/by-nc-nd/4.0/

911 Jørgensen, B.B., Mortensen, P.B., Anderson, F.Ø., Rasmussen, R.A., Jensen, A., 1995.
912 Phosphorous cycling in a coastal marine sediment, Aarhus Bay, Denmark. Limnology
913 and Oceanography 40, 908–917.
914 Kaljo, D. 1996. Diachronous recovery patterns in Early Silurian corals, graptolites, and
915 acritarchs. Geological Society London, Special Publications 102, 127–134.
916 Keeling, R.F., Körtzinger, A., Gruber, N., 2010. Ocean Deoxygenation in a Warming World.
917 Annu. Rev. Mar. Sci. 2, 199–229.
918 Kemp, D.B., Coe, A.L., Cohen, A.S., Schwark, L., 2005. Astronomical pacing of methane
919 release in the Early Jurassic period. Nature 437, 396–399.
920 Kemp, D.B., Coe, A.L.,Cohen, A.S., Weedon, G.P., 2011. Astronomical forcing and
921 chronology of the early Toarcian (Early Jurassic) oceanic anoxic event in Yorkshire,
922 UK. Paleoceanography 26, 1–17.
923 Kemp, D.B., Izumi, K., 2014. Multiproxy geochemical analysis of a Panthalassic margin
924 record of the early Toarcian oceanic anoxic event (Toyora area, Japan).
925 Palaeogeogr. Palaeocol. 414, 332–341.
926 Kirby, M.X., Miller, H.M., 2005. Response of a benthic suspension feeder (*Crassostrea*
927 *virginica* Gmelin) to three centuries of anthropogenic eutrophication in Chesapeake
928 Bay. Estuar. Coast. Shelf S. 62, 679–689.
929 Korte, C., Hesselbo, S.P., Ullmann, C.V., Dietl, G., Ruhl, M., Schweigert, G., Thibault, N.,
930 2015. Jurassic climate governed by ocean gateway. Nature Communications 6:
931 10015.
932 Kristensen, E., 2000. Organic matter diagenesis at the oxic-anoxic interface in coastal marine
933 sediments, with emphasis on the role of burrowing animals. Hydrobiologia 426: 1–24.
934 Levin, L.A., Gage, J., 1998. Relationships between oxygen, organic matter and the diversity
935 of bathyal macrofauna. Deep-Sea Res. Pt. II 45, 129–163.
936 Levinton, J.S., Bambach, R., 1970. Some ecological aspects of bivalve mortality patterns.
937 Am. J. Sci. 268, 97–112.
938 Levinton, J.S., Kelaher, B. 2003. Opposing organizing forces of deposit-feeding marine
939 communities. J. Exp. Mar. Biol. Ecol. 300, 65–82.
940 Levinton, J.S., Bianchi, T. S. 1981. Nutrition and food limitation of deposit feeders. I. The role
941 of microbes in the growth of mud snails. J. Mar. Res. 39, 531–545.
942 Little C.T.S., 1995. The Pliensbachian-Toarcian (Lower Jurassic) extinction event. PhD
943 thesis, Bristol University, Bristol, 144 pp.
944 Little, C.T.S., 1996. The Pliensbachian-Toarcian (Lower Jurassic) extinction event. Pp. 505-
945 512 *in* G. Ryder, D. Fastovsky, and S. Gartner, eds. The Cretaceous-Tertiary event
946 and other catastrophes in Earth history. Geological Society of America, Special
947 Papers, **307**.
948 Little, C.T.S., Benton, M.J., 1995. Early Jurassic Mass Extinction – a Global Long-Term
949 Event. Geology 23, 495–498.
950 Long, C.W., Seitz, R.D., Brylawski, B.J., Lipcius, R.N., 2014. Individual, population, and
951 ecosystem effects of hypoxia on a dominant benthic bivalve in Chesapeake Bay.
952 Ecol. Monogr. 84, 303–327.
953 Lopez, G.R., Levinton, J.S. 1987, Ecology of deposit-feeding animals in marine sediments. Q.
954 Rev. Biol. 62, 235–260.
955 Martindale, R.C., Aberhan, M. 2017. Response of macrobenthic communities to the Toarcian
956 Oceanic Anoxic Event in northeastern Panthalassa (Ya Ha Tinda, Alberta, Canada).
957 Palaeogeogr. Palaeoecol. 478, 103–120.
958 Mattioli, E., Pittet, B., Suan, G., Mailliot, S. 2008. Calcareous nannoplankton changes across
959 the early Toarcian oceanic anoxic event in the western Tethys. Paleoceanography
960 23, 1–17.
961 Mayer, L.M., Schick, L.L., Self, R.F.L., Jumars, P.A., Findlay, R.H., Chen, Z., Sampson, S.
962 1997. Digestive environments of benthic macroinvertebrate guts: enzymes,
963 surfactants and dissolved organic matter. J. Mar. Res. 55, 785-812.
964 McArthur, J.M., Algeo, T.J., van de Schootbrugge, B., Li, Q., Haworth, R.J., 2008. Basinal
965 restriction, black shales, Re-Os dating, and the Early Toarcian (Jurassic) oceanic
966 anoxic event. Paleoceanography 23, 1–22.
967 MacArthur, R.H., 1960. On the relative abundance of species. American Naturalist 94, 25-36.
968 Marinov, V.A., Meledina, S.V., Dzyuba, O.S., Urman, O.S., Yazikova, V., Luchinina, V.A.,
969 Zamirailova, A.G., Fomin, A.N., 2006. Biofacies of Upper Jurassic and Lower
970 Cretaceous sediments of central west Siberia. Stratigr. Geol. Correl. 14, 418–432.

©2020, Elsevier. This manuscript version is made available under the CC-BY-NC-ND 4.0 license http://creativecommons.org/licenses/by-nc-nd/4.0/

971 Martin, K.D., 2004. A re-evaluation of the relationship between trace fossils and dysoxia.
972 Geological Society London, Special Publications 228, 141-156.
973 Meysman, F.J.R., Middelburg, J.J., Heip, C.H.R., 2006. Bioturbation: a fresh look at Darwin's
974 last idea. Trends Ecol. Evol. 21, 688–694.
975 Morris, K.A., 1979. A classification of Jurassic marine shale sequences: An example from the
976 Toarcian (Lower Jurassic) of Great Britain. Palaeogeogr. Palaeocol. 26, 117–126.
977 Moss, D. K., Ivany, L. C., Judd, E. J., Cummings, P. W., Bearden, C. E., Kim, W.-J., Artruc, E.
978 G., Driscoll, J. R. 2016. Lifespan, growth rate, and body size across latitude in
979 marine Bivalvoa, with implications for Phanerozoic evolution. Proc. R. Soc. B 283, 1–
980 7.
981 Nakaoka, M, Matsui, S., 1994. Annual variation in the growth arte of *Yoldia notabilis* (Bivalvia:
982 Nuculanidae) in Otsuchi Bay, northeastern Japan, analyzed using shell microgrowth
983 patterns. Mar. Biol. 119, 397–404.
984 Nikitenko, B., Shurygin, B., Mickery, M., 2008. High resolution stratigraphy of the Lower
985 Jurassic and Aalenian of Arctic regions as the basis for detailed palaeobiogeographic
986 reconstructions. Norw. J. Geol. 88, 267–278.
987 Nikitenko, B.L., Shurygin, B.N., 1992. Lower Toarcian black shales and Pliensbachian-
988 Toarcian crisis of the biota of Siberian paleoseas. Pp. 39-44 *in* D. E. Thurston, and K.
989 Fujita, eds. 1992 Proceedings of the International Conference on Arctic Margins. U.S.
990 Department of the Interior, Minerals Management Service, Alaska Outer Continental
991 Shelf Region, Anchorage, Alaska.
992 Nilsson, H.C., Rosenberg, R., 1994. Hypoxic response of two marine benthic communities.
993 Mar. Ecol-Prog. Ser. 115, 209–217.
994 Norrko, A., Bonsdorff, E., 1996. Altered benthic prey-availability due to episodic oxygen
995 deficiency caused by drifting algal mats. Mar. Ecol. 17, 355–372.
996 Olafsson, E.B., 1986. Density dependence in suspension-feeding and deposit-feeding
997 populations of the bivalve *Macoma balthica*: A field experiment. J. Anim. Ecol. 55,
998 517–526.
999 Palliani, R.B., Mattioli, E., Riding, J.B., 2002. The response of marine phytoplankton and
1000 sedimentary organic matter to the early Toarcian (Lower Jurassic) oceanic anoxic
1001 event in northern England. Mar. Micropaleontol. 46, 223–245.
1002 Pearce, C.R., Cohen, A.S., Coe, A.L., Burton, K.W., 2008. Molybdenum isotope evidence for
1003 global ocean anoxia coupled with perturbations to the carbon cycle during the early
1004 Jurassic. Geology 36, 231–234.
1005 Pearson, T.H., Rosenberg, R., 1978. Macrobenthic succession in relation to organic
1006 enrichment and pollution of the marine environment. Oceanogr. Mar. Biol. 16, 229–
1007 311.
1008 Powers, S.P., Peterson, C.H., Christian, R.R., Sullivan, E. Powers, M.J. Bishop, M.J.,
1009 Buzzelli, C.P., 2005. Effects of eutrophication on bottom habitat and prey resources
1010 of demersal fishes. Mar. Ecol-Prog. Ser. 302, 233–243.
1011 Prager, M.H., Saila, S.B., Recksiek, C.W., 1994. FISHPARM: A Microcomputer Program for
1012 Parameter Estimation of Nonlinear Models in Fishery Science.
1013 Raiswell, R., Bottrell, S.H., Al-Biatty, H.J., Tan, M.M., 1993. The influence of bottom water
1014 oxygenation and reactive iron content on sulfur incorporation into bitumens from
1015 Jurassic marine shales. Am. J. Sci. 293, 569–596.
1016 Rawson, P.F., Wright, J.K., 1995. Jurassic of the Cleveland Basin, North Yorkshire. Pp. 173–
1017 208 *in* Taylor, P. D., ed Field Geology of the British Jurassic. Geological Society,
1018 London.
1019 Riedel, B., Pados, T., Schiemer, L., Steckbauer, A., Haselmair, A., Zuschin, M., Stachowitsch,
1020 M., 2014. Effect of hypoxia and anoxia on invertebrate behaviour: ecological
1021 perspectives from species to community level. Biogeosciences 11, 1491–1518.
1022 Riegraf, W., 1982. The Bituminous Lower Toarcian at the Truc de Balduc near Mende
1023 (Departement de la Lozere, S-France). Pp. 506-511 *in* G. Einsele, and A. Seilacher,
1024 eds. Cyclic and event stratification. Springer, Berlin.
1025 Rodriguez-Tovar, F.J., Reolid, M. 2014. Environmental conditions during the Toarcian
1026 Oceanic Anoxic Event (T-OAE) in the westernmost Tethys: influence of the regional
1027 context on a global phenomenon. Bulletin of Geosciences 88, 697-712.
1028 Röhl, H.-J., 1998. Hochauflösende palökologische und sedimentologische Untersuchungen
1029 im Posidonienschiefer (Lias [epsilon]) von SW-Deutschland. Tübinger
1030 Geowissenschaftliche Arbeiten A 47, 1–170.

©2020, Elsevier. This manuscript version is made available under the CC-BY-NC-ND 4.0 license http://creativecommons.org/licenses/by-nc-nd/4.0/

1031 Röhl, H.-J., Schmid-Röhl, A., Oschmann, W., Frimmel, A., Schwark, L., 2001. The Posidonia
1032 Shale (lower Toarcian) of SW Germany an oxygen-depleted ecosystem controlled by
1033 sea level and palaeoclimate. Palaeogeogr. Palaeoecol. 165, 27–52.
1034 Rosenberg, R., Loo, L.O., 1988. Marine eutrophication induced oxygen deficiency: effects on
1035 soft bottom fauna, Western Sweden. Ophelia 29, 213–225.
1036 Rosenberg, R., Hellman, B., Johansson, B. 1991. Hypoxic tolerance of marine benthic fauna.
1037 Mar. Ecol-Prog. Ser. 79, 127–131.
1038 Ruban, D. 2004. Diversity dynamics of Early-Middle Jurassic brachiopods of Caucasus, and
1039 the Pliensbachian-Toarcian mass extinction. Acta Palaeontol Pol 49, 275–282.
1040 Schöne, B.R., Houk, S.D., Freyre Castro, A.D., Fiebig, J., Oschmann, W., 2005. Daily Growth
1041 Rates in Shells of *Arctica islandica*: Assessing Sub-seasonal Environmental Controls
1042 on a Long-lived Bivalve Mollusk. Palaios 20, 78–92.
1043 Seitz, R.D., Marshall Jr, L.S.A., Hines, H., Clark, K.L., 2003. Effects of hypoxia on predator-
1044 prey dynamics of the blue crab *Callinectes sapidus* and the Baltic clam *Macoma*
1045 *balthica* in Chesapeake Bay. Mar. Ecol-Prog. Ser. 257, 179–188.
1046 Sellwood, B.W., 1972. Regional environmental changes across a lower Jurassic stage-
1047 boundary in Britain. Palaeontology 15, 125-157.
1048 Shurygin, B.N., 1983. Toarskiye "Ledy" (*Dacryomya*) na severe Sibiri (Toarcian "*Leda*"
1049 (*Dacryomya*) of northern Siberia) Trudy Instituta Geologii i Geofiziki (Novosibirsk)
1050 538, 156–167.
1051 Smith, A.B., Jeffery, C.H., 1998. Selectivity of extinction among sea urchins at the end of the
1052 Cretaceous period. Nature 392, 69–71.
1053 Smith, F.A., and K.S. Lyons. 2013. Animal body size: Linking patterns and process across
1054 space, time and taxonomic group. University of Chicago Press, Chicago, USA.
1055 Sokołowski, A., Pawlikowski, K., Wołowicz, M., Garcia, P., Namieśnik, J., 2008. Shell
1056 deformations in the Baltic clam *Macoma balthica* from southern Baltic Sea (the Gulf
1057 of Gdansk): Hypotheses on environmental effects. Ambio 37, 93–100.
1058 Stanley, S.M., 1970. Relation of shell form to life habits of the Bivalvia (Mollusca). Geol. Soc.
1059 Am. Mem. 125, 1–282.
1060 Stanley, S.M., 1981. Infaunal survival: Alternative functions of shell ornamentation in the
1061 Bivalvia (Mollusca). Paleobiology 7, 384–393.
1062 Stramma, L., Schmidtko, S., Levin, L.A., Johnson, G.C., 2010. Ocean oxygen minima
1063 expansions and their biological impacts. Deep-Sea Res. Pt. I 57, 587–595.
1064 Suan, G., Mattioli, E., Pittet, B., Mailliot, S., Lécuyer, C., 2008. Evidence for major
1065 environmental perturbation prior to and during the Toarcian (Early Jurassic) oceanic
1066 anoxic event from the Luisitanian Basin. Paleoceanography 23, 1–14.
1067 Tallqvist, M., 2001. Burrowing behaviour of the Baltic clam *Macoma balthica*: effects of
1068 sediment type, hypoxia and predator presence. Mar. Ecol-Prog. Ser. 212, 183–191.
1069 Tate, R., Blake, J.F., 1876. The Yorkshire Lias. John Van Voorst, London.
1070 Taylor, D., Egglestone, D.B., 2000. Effects of hypoxia on an estuarine predator-prey
1071 interaction: mutual interference and foraging behaviour of the blue crab (*Callinectes*
1072 *sapidus*) on infaunal clam prey (*Mya arenaria*). Mar. Ecol-Prog. Ser. 196, 221–237.
1073 Thibault, N., Ruhl, M., Ullman, C.V., Korte, C., Kemp, D.B., Grocke, D.R., Hesselbo, S.P.,
1074 2018. The wider context of the Lower Jurassic Toarcian oceanic anoxic event in
1075 Yorkshire coastal outcrops, UK. P. Geologist. Assoc. 129, 372–391.
1076 Thompson, J.K., Nichols, F.H., 1988. Food availability controls seasonal cycle of growth in
1077 *Macoma balthica* (L.) in San Francisco Bay, California. J. Exp. Mar. Biol. Ecol. 116,
1078 43–61.
1079 Twitchett, R.J., 2006. The palaeoclimatology, palaeoecology and palaeoenvironmental
1080 analysis of mass extinction events. Palaeogeogr. Palaeoecol. 232, 190–213.
1081 Ullmann, C.V., Thibault, N., Ruhl, M., Hesselbo, S.P., Korte, C., 2014. Effect of a Jurassic
1082 oceanic anoxic event on belemnite ecology and evolution. P. Ntl. Acad. Sci. USA
1083 111, 10073–10076.
1084 Urbanek, A., 1993. Biotic crises in the history of upper Silurian graptoloids: a palaeobiological
1085 model. Historical Biology 7, 29–50.
1086 Correia, V.F., Riding, J.B., Duarte, L.V., Fernandes, P., Pereira, Z. 2017. The palynological
1087 response to the Toarcian Oceanic Anoxic Event (Early Jurassic) at Peniche, western
1088 Portugal. Mar. Micropaleontol. 137, 46–63.
1089 von Bertalanffy, L. 1938. A quantitative theory of organic growth (inquiries on growth laws II).
1090 Human Biology 10, 181- 213.

©2020, Elsevier. This manuscript version is made available under the CC-BY-NC-ND 4.0 license http://creativecommons.org/licenses/by-nc-nd/4.0/

Vörös, A. 2002. Victims of the Early Toarcian anoxic event: the radiation and extinction of Jurassic Koninckinidae (Brachiopoda). Lethaia 35, 345–357.
Ward, P.D., Haggart, J.W., Carter, E.S., Wilbur, D., Tipper, H.W., Evans, T., 2004. Sudden productivity collapse associated with the Triassic–Jurassic boundary mass extinction. Science 292, 1148–1151.
Watson, J.S., 1982. The occurrence of *Discinisca* on *Dacryomya ovum*: An example of commensalism from the Upper Lias of Yorkshire. P Yorks. Geol. Soc. 44, 45–51.
Welsh, D.T., 2003. It's a dirty job but someone has to do it: the role of marine benthic macrofauna in organic matter turnover and nutrient recycling to the water column. Chemistry and Ecology 19, 321–342.
Weston, D.P., 1990. Quantitative examination of macrobenthic community changes along an organic enrichment gradient. Marine Ecology Progress Series 61, 233–244.
Wright, P., Cherns, L., Hodges, P. 2003. Missing molluscs: field testing taphonomic loss in the Mesozoic through early large-scale aragonite dissolution. Geology 31, 211–214.
Zakharov, V.A., Shurygin, B.N., Il'ina, V.I., Nikitenko, B.L., 2006. Pliensbachian-Toarcian biotic turnover in north Siberia and the Arctic region. Stratigraphy and Geological Correlation 14, 399–417.

Figure captions

Fig. 1. Field study area. A. Map of the UK. Grey inset boxes show sites of *M. balthica* (northwest UK) and *D. ovum* collection (northeast UK; detail covered by B). B. Map of the Cleveland Basin showing the Lower Jurassic outcrops, showing Peak Fault (N-S oriented) to the east, and the Vale of Pickering and the Howardian – Flamborough Fault Belt (E-W oriented) to the south (modified from Rawson and Wright, 1995). Locations of the exposure from which the samples were collected between Whitby and Saltwick Bay, NE Yorkshire, UK are shown together with four other key localities with extensive early Toarcian exposure.

Fig. 2. Specimens of *Dacryomya ovum* from Saltwick Bay, N Yorkshire, UK showing A. Measurement of shell length (S-L where S is the posterior and L is the anterior end of the shell), shell height (U-V where U is umbo and V the ventral side of the shell). Additional measurements used to calculate the three deformation indices include: UA, UB, UC, UD, UE, UF, UG, UH, UI and US are the distances, at the posterior end, from the umbo to the shell margin; each line marks one tenth of the total angle between UV and US. UJ, UK and UL are the distances, on the anterior

©2020, Elsevier. This manuscript version is made available under the CC-BY-NC-ND 4.0 license http://creativecommons.org/licenses/by-nc-nd/4.0/

1127 end, between the umbo and the shell margin with each line representing one third of
1128 the total angle between UV and UL. B. Complete uncompacted *D. ovum* viewed from
1129 the right with arrows indicating annuli. C–E Complete uncompacted *D. ovum* (h/i =
1130 0.07, 1.16, 1.20) showing varying degrees of posterior elongation (SDI3 = 1.03, 1.02,
1131 0.97; low values indicating greater elongation) and flexure (SDI1 = 1.05, 1.04, 0.97,
1132 respectively; low values indicating high flexure). F. Compacted *D. ovum* showing one
1133 valve slipped inside of the other (h/i = 1.84), and G. same specimen view of the left
1134 valve showing small shell fractures. H. Dorsal view of uncompacted *D. ovum*
1135 specimen shown in B. Supplementary Table S3 for raw data.
1136
1137 **Fig. 3.** Stratigraphic log of the upper Mulgrave Shale and lower Alum Shale
1138 members. Ammonite biostratigraphy, lithology, bed numbers and thicknesses are
1139 from Howarth (1962). The Alum Shale Member is unconformably overlain by middle
1140 Jurassic sandstones. Stratigraphic height (m) is above base of the *Cleviceras*
1141 *exaratum* subzone. A. *D. ovum* shell compaction (h/i), proportion of internal moulds,
1142 and proportion orthogonal to bedding plane in each assemblage. Skew of *D. ovum*
1143 shell length and length frequency distributions throughout the species range (this
1144 study). Shell length frequency histograms for *Dacryomya ovum* from each of the 30
1145 stratigraphic levels. † = indicates that LFDs may underestimate shell length by a
1146 small (<3 mm) amount due to the greater proportion of internal moulds in the sample.
1147 B. Shell length frequency histograms for the dominant bivalve species present in the
1148 *bifrons*, *falciferum* and *exaratum* subzones of the Whitby Mudstone Formation,
1149 Yorkshire, UK. For comparison shell length frequency histograms for present-day
1150 bivalves K-strategist and opportunists e.g. *Mya arenaria* (pooled data from 24
1151 samples) and *Mulinia lateralis* (time averaged death assemblage), respectively (data
1152 from Emerson et al. 1988, Levinton and Bambach 1970). From top: *Dacryomya*
1153 *ovum* in high TOC assemblages, low TOC assemblages and across all stratigraphic
1154 levels sampled (this study); *Psuedomytiloides dubius* from the *falciferum* (post-OAE)

©2020, Elsevier. This manuscript version is made available under the CC-BY-NC-ND 4.0 license http://creativecommons.org/licenses/by-nc-nd/4.0/

and *exaratum* (during OAE) subzones, and *Bositra radiata* from the *tenuicostatum* Subzone (the onset of the OAE; Caswell and Coe 2013). Ammonite zone and subzone abbreviations: *H. falcif.* = *Harpoceras falciferum* (J. Sowerby), and *C. crass.* = *Catacoeloceras crassum* Young and Bird.

Fig. 4. Stratigraphic log of the upper Mulgrave Shale and lower Alum Shale members exposed between Whitby and Saltwick Bay. Ammonite biostratigraphy and lithology are as for Fig. 3. Total organic carbon (TOC) data are combined from Harding (2004) and McArthur et al. (2008). *Dacryomya ovum* mean shell length (± standard error), abundance, flexure (SDI1), elongation (SDI3 ± standard error), and shell clustering (this study). * = shell length in the *fibulatum* Subzone may be underestimated by ~3 mm (due to most measurements being based on internal moulds that lack a shell). Species abundances for benthic macrofossils are from Little (1995, 1996) and Caswell et al. (2009) and include seven bivalve species (*D. ovum, P. dubius, M. substriata, B. buchi, G. donaciformis, O. inequivalve* and *L. hisingeri*), two brachiopods (*L. longovicensis* and *D. papyracea*), the crinoid *C. wuerttenbergicus* and the gastropod *P. expansus*.

Fig. 5. Growth curves with shell height at each growth increment for six specimens of *Dacryomya ovum* collected from four different stratigraphic heights (each line represents one individual specimen) in the Whitby Mudstone Formation, Yorkshire, UK. The population growth rate (ω) for the *D. ovum* specimens ranged from 2.84 to 6.80.

©2020, Elsevier. This manuscript version is made available under the CC-BY-NC-ND 4.0 license http://creativecommons.org/licenses/by-nc-nd/4.0/

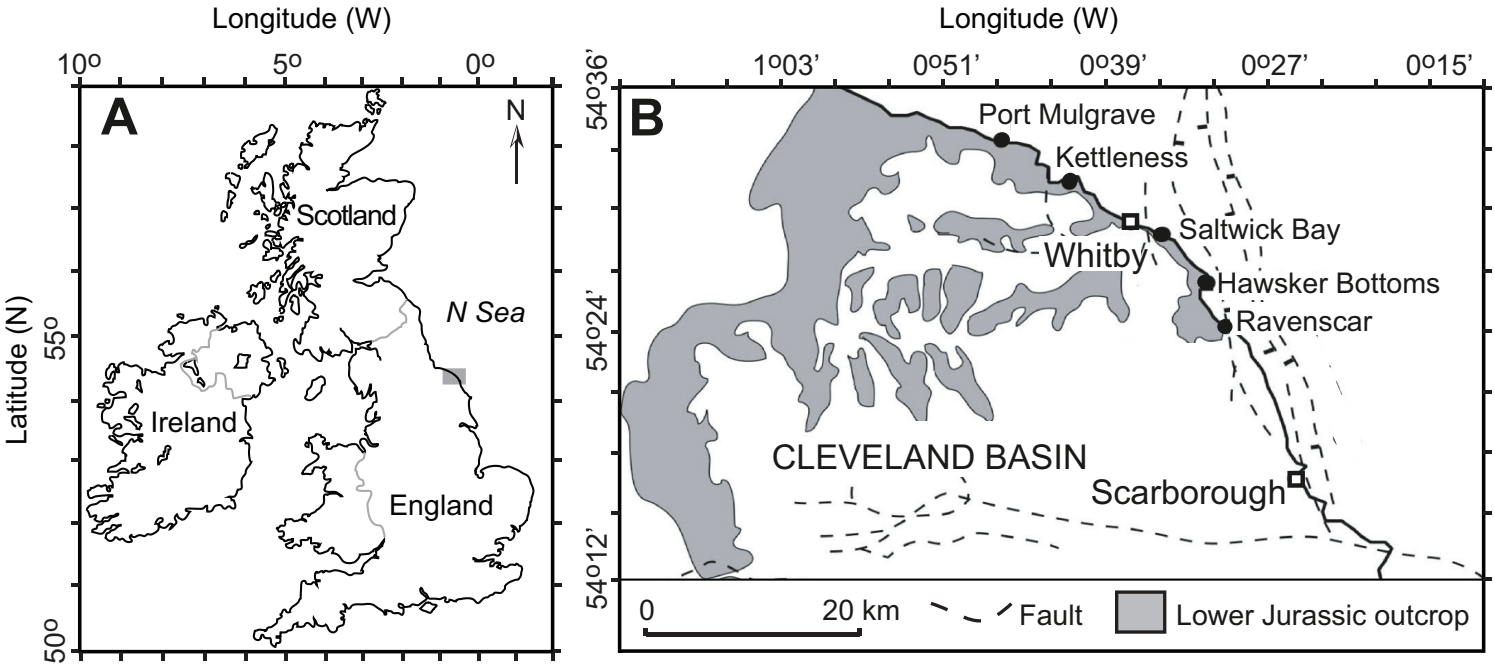

Fig. 1 Caswell and Dawn

©2020, Elsevier. This manuscript version is made available under the CC-BY-NC-ND 4.0 license http://creativecommons.org/licenses/by-nc-nd/4.0/

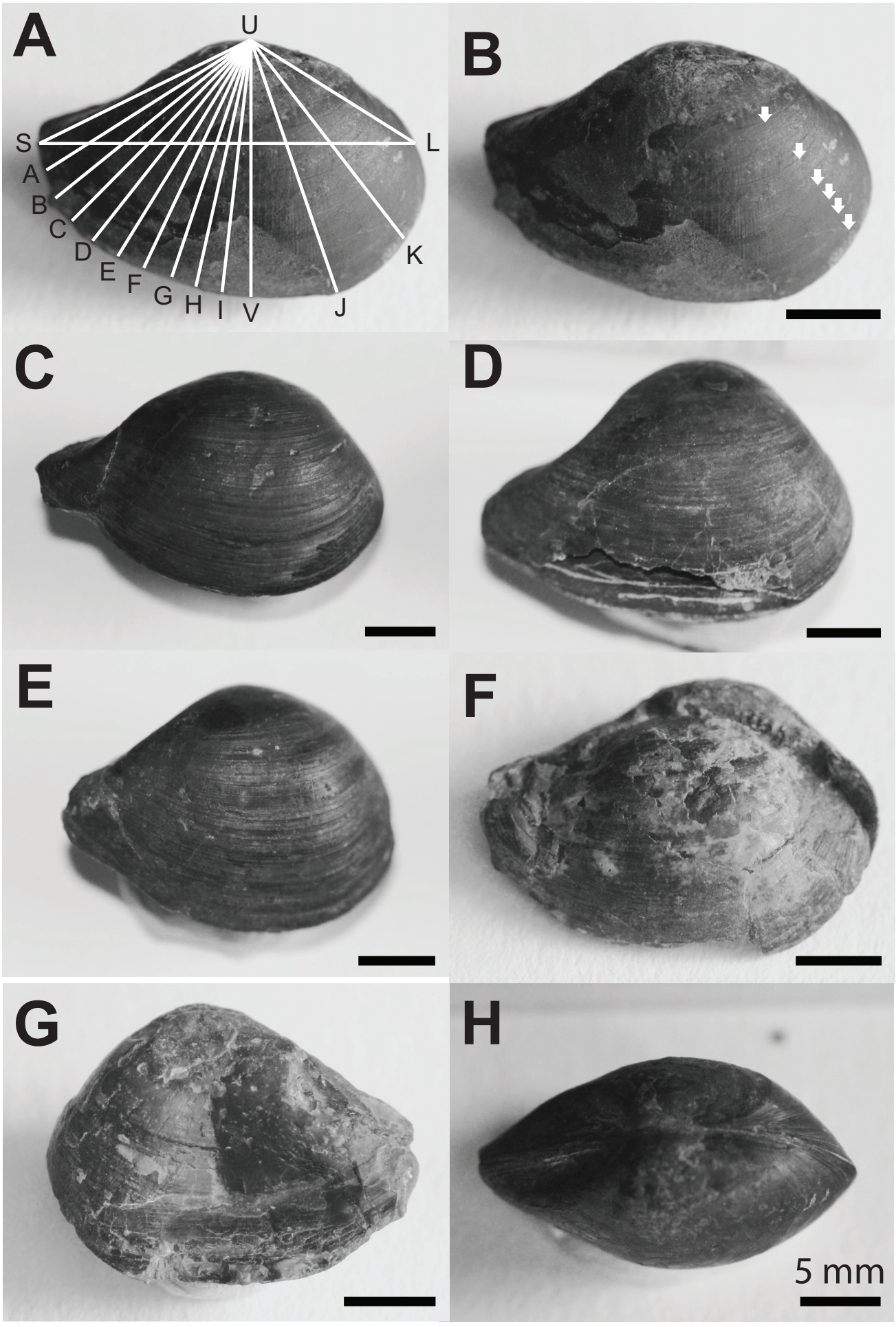

Fig. 2 Caswell and Dawn

©2020, Elsevier. This manuscript version is made available under the CC-BY-NC-ND 4.0 license http://creativecommons.org/licenses/by-nc-nd/4.0/

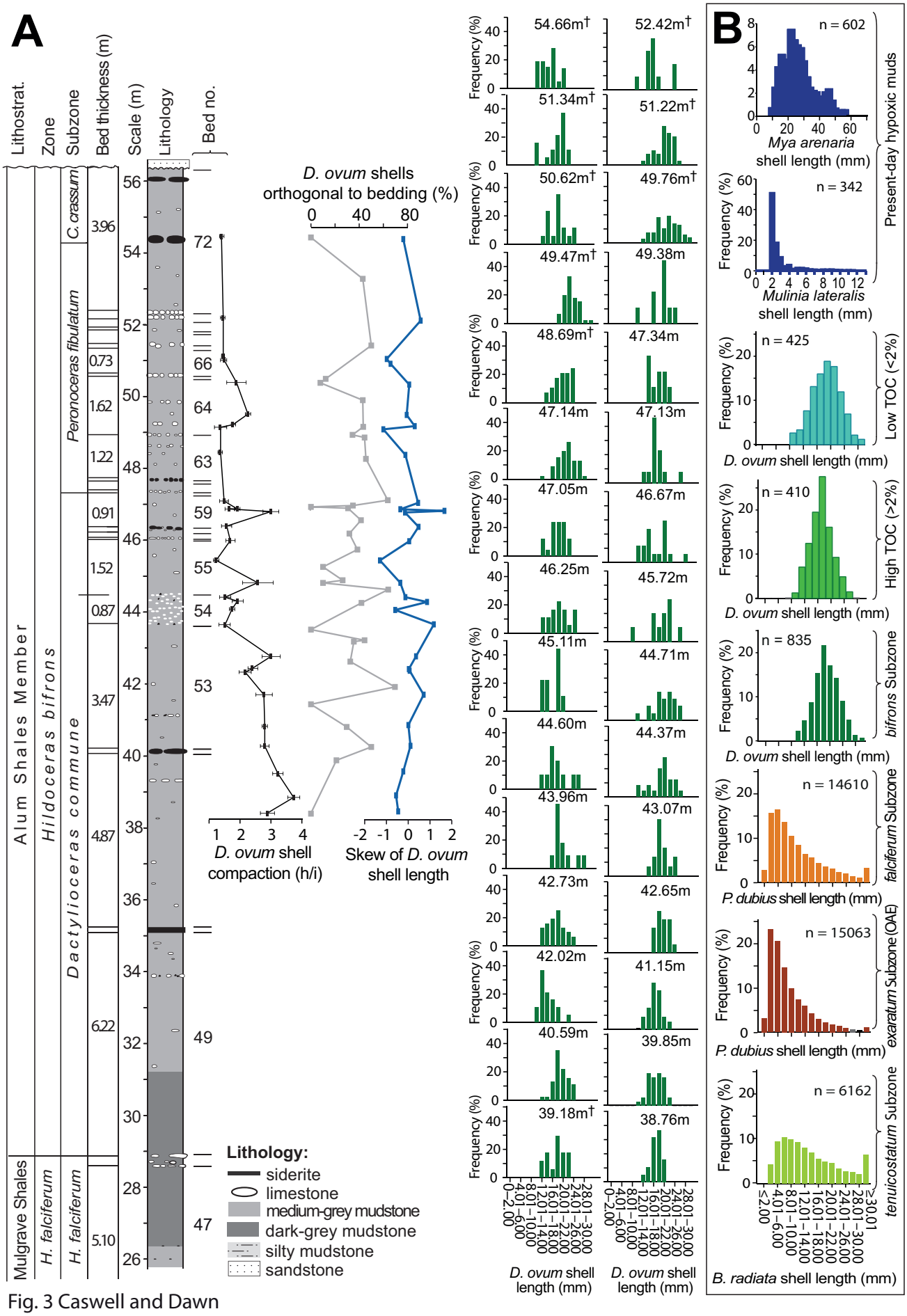

Fig. 3 Caswell and Dawn

©2020, Elsevier. This manuscript version is made available under the CC-BY-NC-ND 4.0 license http://creativecommons.org/licenses/by-nc-nd/4.0/

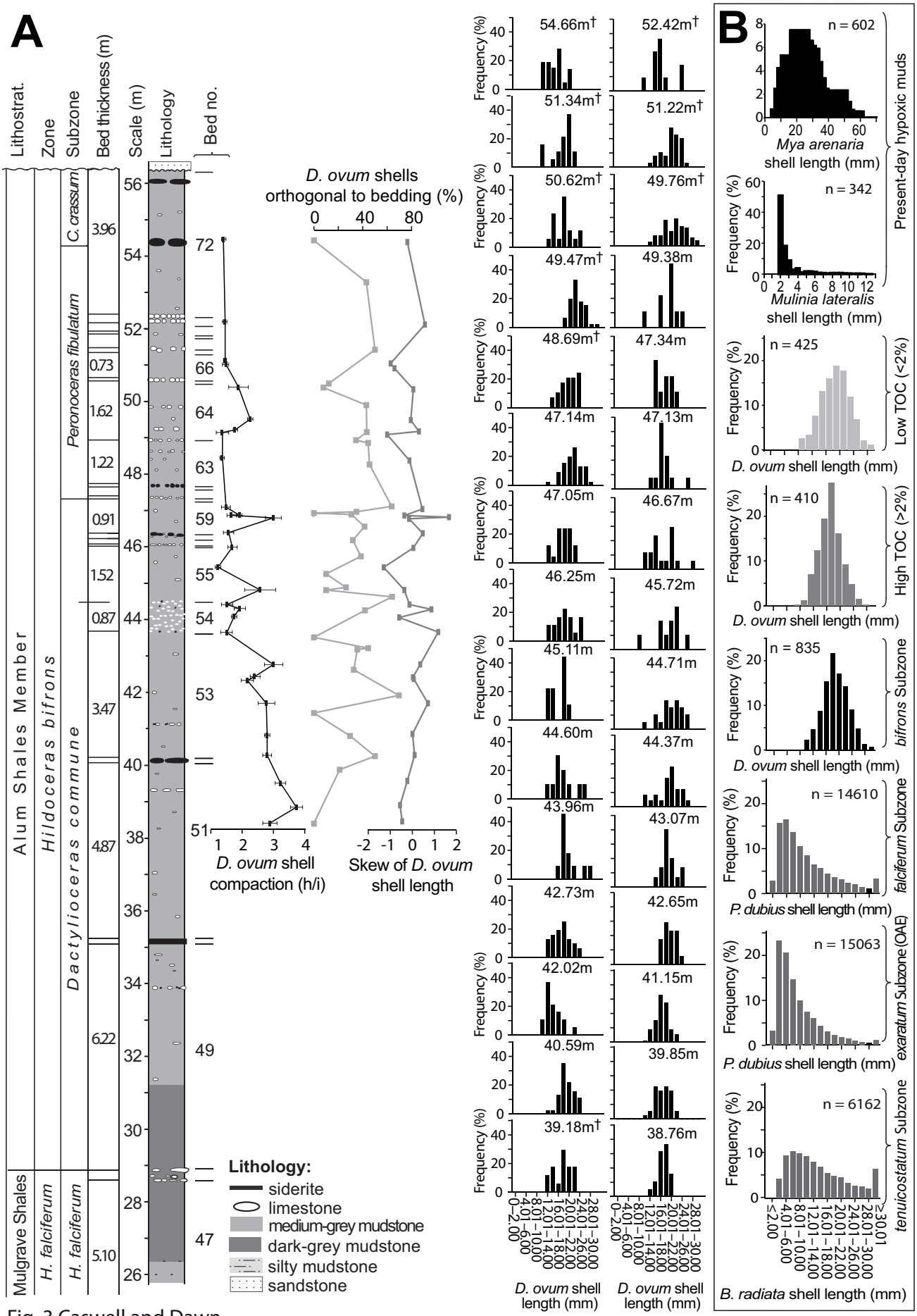

Fig. 3 Caswell and Dawn

©2020, Elsevier. This manuscript version is made available under the CC-BY-NC-ND 4.0 license http://creativecommons.org/licenses/by-nc-nd/4.0/

Fig. 4 Caswell and Dawn

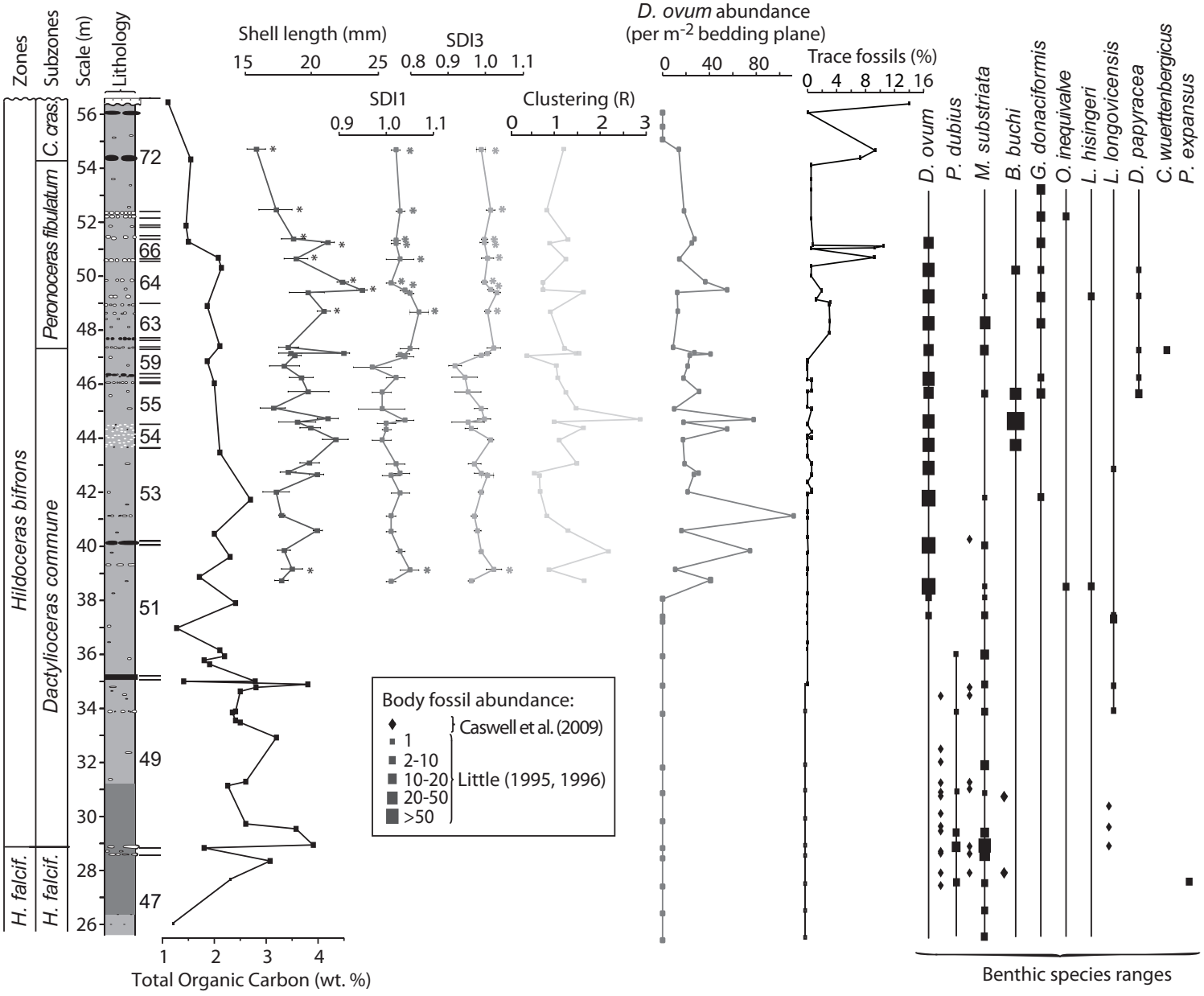

©2020, Elsevier. This manuscript version is made available under the CC-BY-NC-ND 4.0 license http://creativecommons.org/licenses/by-nc-nd/4.0/

Fig. 4 Caswell and Dawn

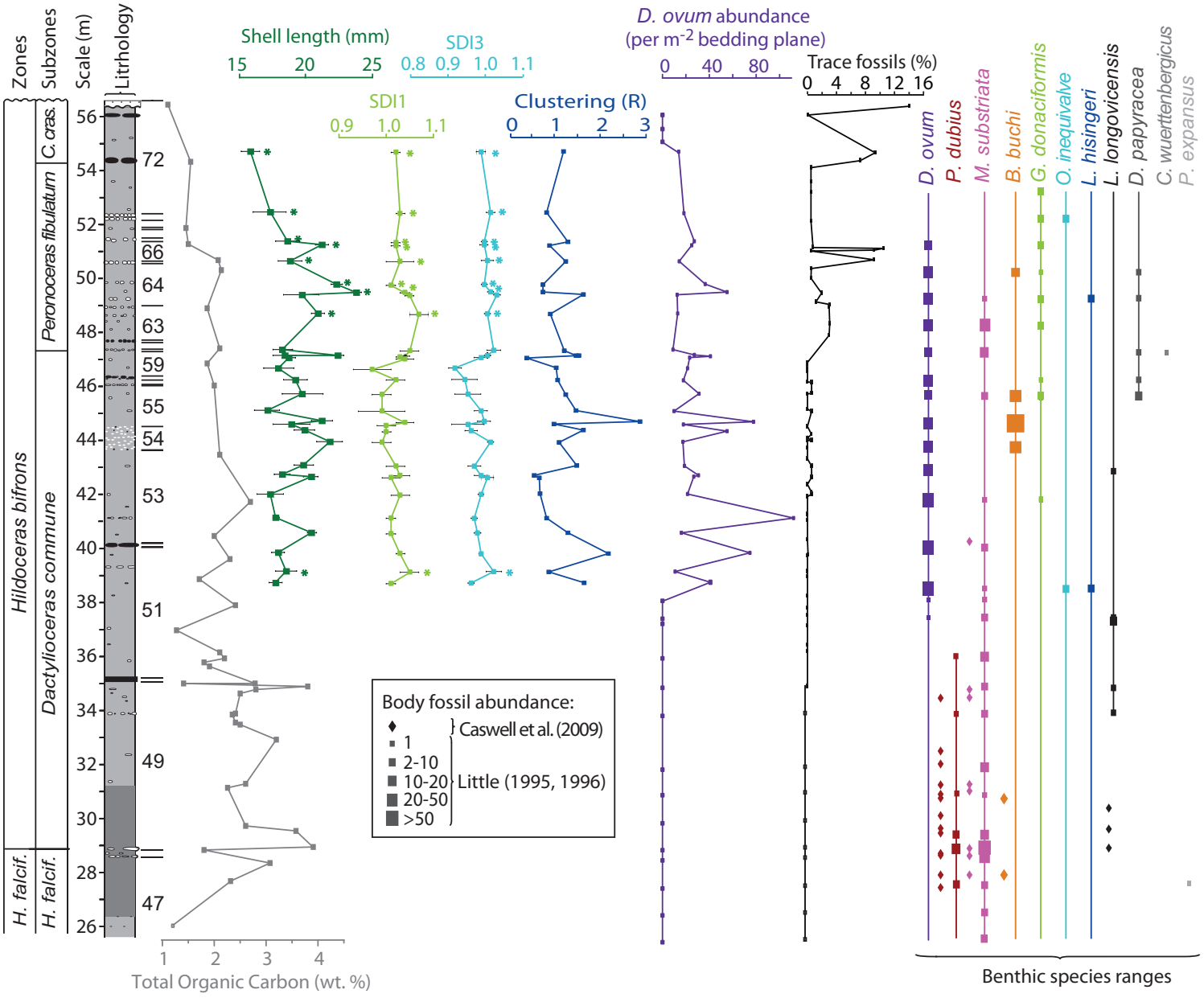

©2020, Elsevier. This manuscript version is made available under the CC-BY-NC-ND 4.0 license http://creativecommons.org/licenses/by-nc-nd/4.0/

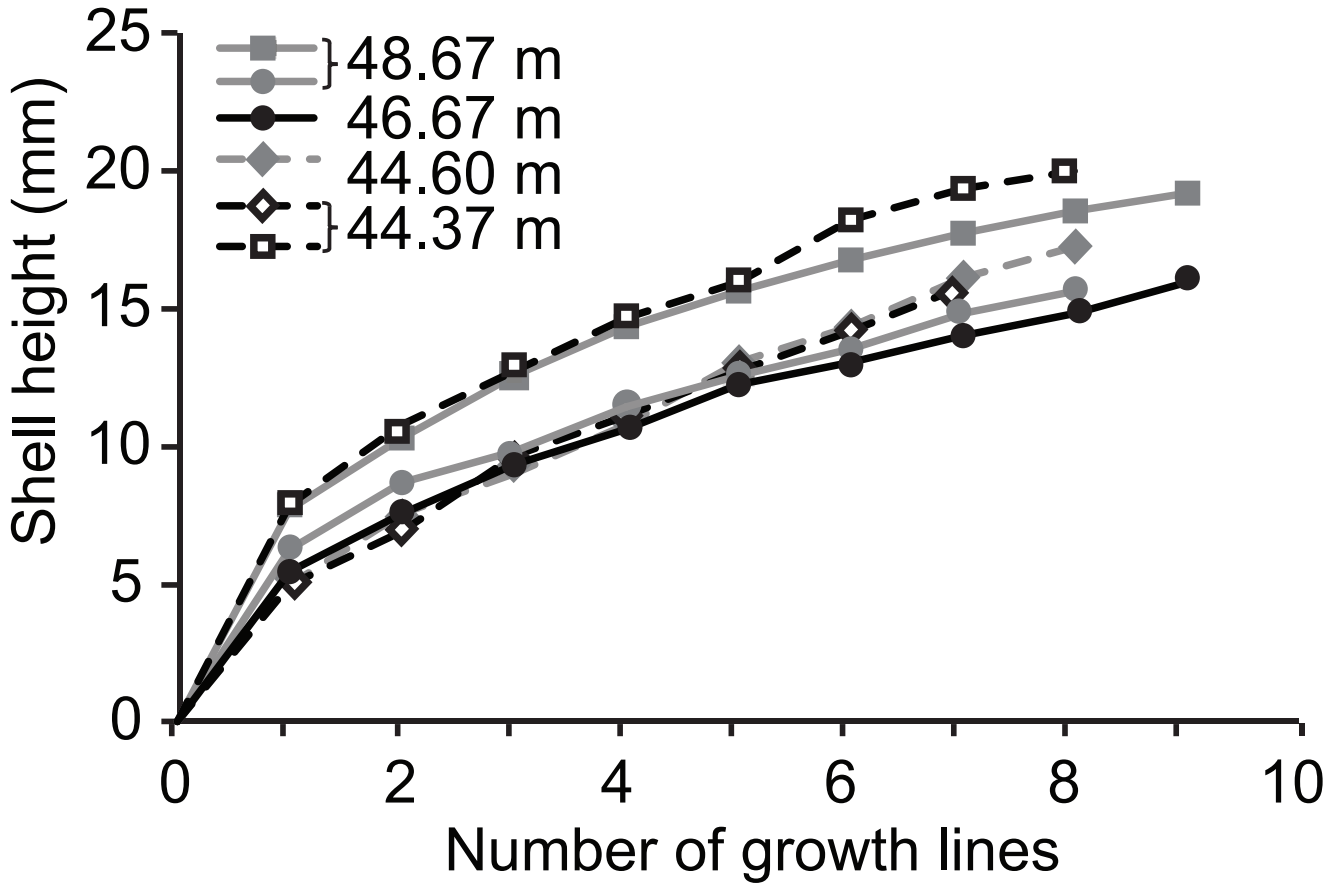

Fig. 5 Caswell and Dawn

©2020, Elsevier. This manuscript version is made available under the CC-BY-NC-ND 4.0 license http://creativecommons.org/licenses/by-nc-nd/4.0/

Table 1. Median *D. ovum* shell morphometrics from strata with high (>2%) and low (<2%) total organic carbon (TOC, wt. %), and statistical results for low and high TOC assemblage comparisons.

Group	Mean (± IQR)			Median (± IQR‡)		
	Shell length (mm)	**Shell width (mm)**	**Shell inflation (mm)**	**SDI†1**	**SDI2**	**SDI3**
TOC ≤2%	21.90 ± 5.20	14.90 ± 3.80	8.50 ± 4.45	1.03 ±0.08	1.02 ± 0.00	1.02 ± 0.07
TOC ≥2%	19.08 ± 3.95	14.11 ± 3.36	5.30 ± 3.25	1.01 ±0.06	1.03 ± 0.00	0.99 ± 0.07
MW test§	Z = -7.63, p < 0.001*	Z = -3.63, p < 0.006*	Z = -10.42 p<0.001*	Z = -3.52, p = 0.002*	Z = -1.07 p = 0.284	Z = -4.43, p < 0.001*

*Indicates statistical significance at p<0.05; †SDI = Shell Deformation Index, ‡IQR = Interquartile Range, §MW = Mann-Whitney U-tests.

©2020, Elsevier. This manuscript version is made available under the CC-BY-NC-ND 4.0 license http://creativecommons.org/licenses/by-nc-nd/4.0/

Table 2. Results of stepwise multiple regression with mean *D. ovum* shell length, mean shell width and maximum shell length (for which two models are presented), and five proxies for primary production (TOC), palaeotemperature ($\partial^{18}O$) and palaeoredox ([U], [Mo], TOC/TS). Only significant variables are shown.

Regression model*	R^2	B (± SE)†	ß‡	t	p§	Tolerance	VIF	DW
Mean shell length								
TOC	**0.34**	**5.88 (± 2.36)**	**0.58**	**2.50**	**0.028**	**1.00**	**1.00**	**1.57**
TOC/TS			0.11	.31	p>0.05	0.48	2.10	-
[Mo]			0.26	1.1	p>0.05	0.90	1.11	-
[U]			-0.12	-0.48	p>0.05	0.97	1.04	-
$\partial^{18}O$			-0.28	-1.0	p>0.05	0.70	1.44	-
Mean shell width								
TOC	**0.44**	**3.72 (± 1.21)**	**0.66**	**3.07**	**0.010**	**1.00**	**1.00**	**2.23**
TOC/TS			0.12	0.38	p>0.05	0.48	2.10	-
[Mo]			0.07	0.30	p>0.05	0.90	1.11	-
[U]			-0.13	-0.13	p>0.05	0.97	1.04	-
$\partial^{18}O$			0.08	0.31	p>0.05	0.70	1.44	-
Max shell length								
TOC/TS	**0.37**	**12.00 (± 4.52)**	**0.61**	**2.66**	**0.021**	**1.00**	**1.0**	**2.29**
TOC			0.30	0.88	p>0.05	0.48	2.10	-
[Mo]			0.16	0.70	p>0.05	0.99	1.00	-
[U]			0.25	0.64	p>0.05	0.36	2.79	-
$\partial^{18}O$			-0.15	0.61	p>0.05	0.97	1.03	-

*Tolerance, VIF, and Durbin Watson statistics (>0.2, <10 and between 1.5-2.5, respectively) suggest no multi-colinearity or autocorrelation in the models. †B (± standard error) model coefficient indicates contribution to the model: so a 1 unit change in the predictor variable produces a change in shell size equivalent to B; ‡ ß is the standardised model coefficient. §p<0.05 confirms there is a significant relationship with the predictor variable;

©2020, Elsevier. This manuscript version is made available under the CC-BY-NC-ND 4.0 license http://creativecommons.org/licenses/by-nc-nd/4.0/

Table 3. Comparisons of maximum shell length, height, inflation, height/length (H/L) and mean height/inflation (H/I) of different Jurassic *Dacryomya* species.

Age	Species	N*	Max. shell dimensions (mm)			Max. H/L	Mean H/I
			L	H	I		
Sinemurian§	*D. heberti*	48	4.9	3.5	3.6	0.71	0.97
Pliensbachia§	*D. gaveyi*	33	8.7	6.0	5.1	0.69	1.18
Toarcian‡	*D. ovum*	629	19.2	15.7	11.5	0.72	2.24†
Oxfordian#	*D. roederi*	11	7.7	4.7	-	0.61	-

*N = sample size, hyphen indicates no data were available. †Mean reflects a mixture of compacted and uncompacted shells; those that showed no evidence of compaction had a H/I ranging from 1.10 to 1.30. ‡Data from this study, §Hodges (2000), and #Delvene (2000).

©2020, Elsevier. This manuscript version is made available under the CC-BY-NC-ND 4.0 license http://creativecommons.org/licenses/by-nc-nd/4.0/

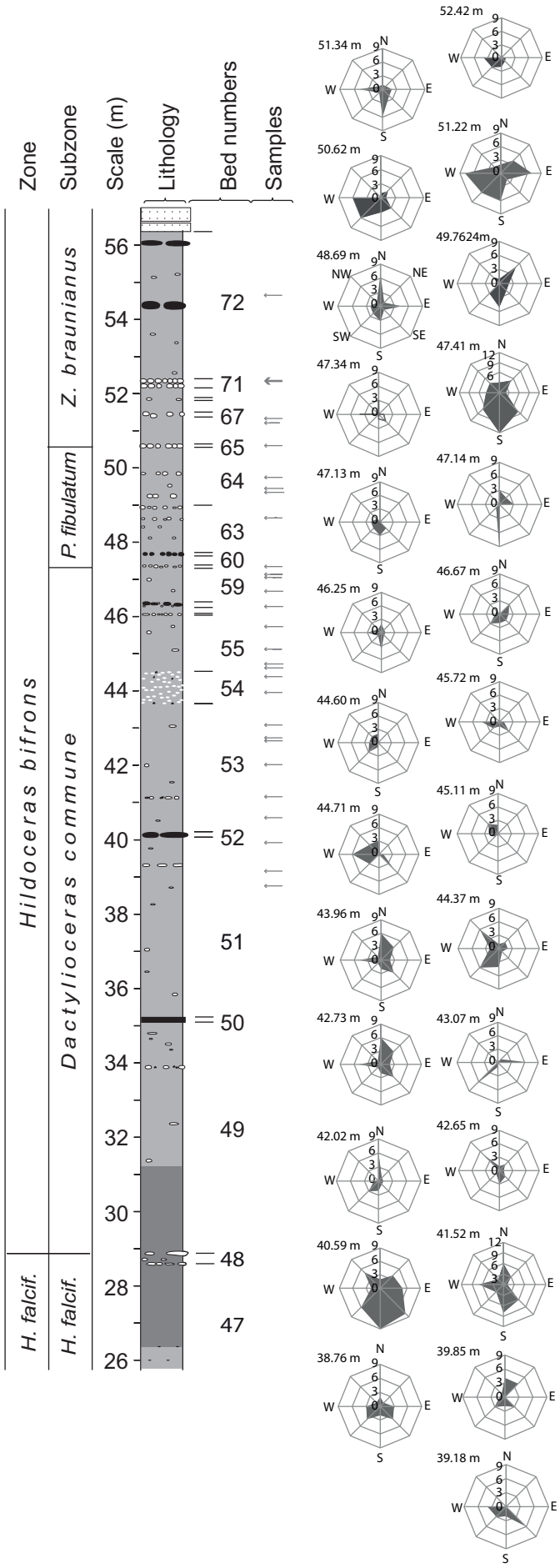

Fig. S1. Stratigraphic log showing compass orientations of the posterior ends of *Dacryomya ovum* shells within each assemblage sampled (stratigraphic positions of the 30 assemblages are indicated with arrows). Biostratigraphy, lithology and bed numbers are as for Fig. 3.

©2020, Elsevier. This manuscript version is made available under the CC-BY-NC-ND 4.0 license http://creativecommons.org/licenses/by-nc-nd/4.0/

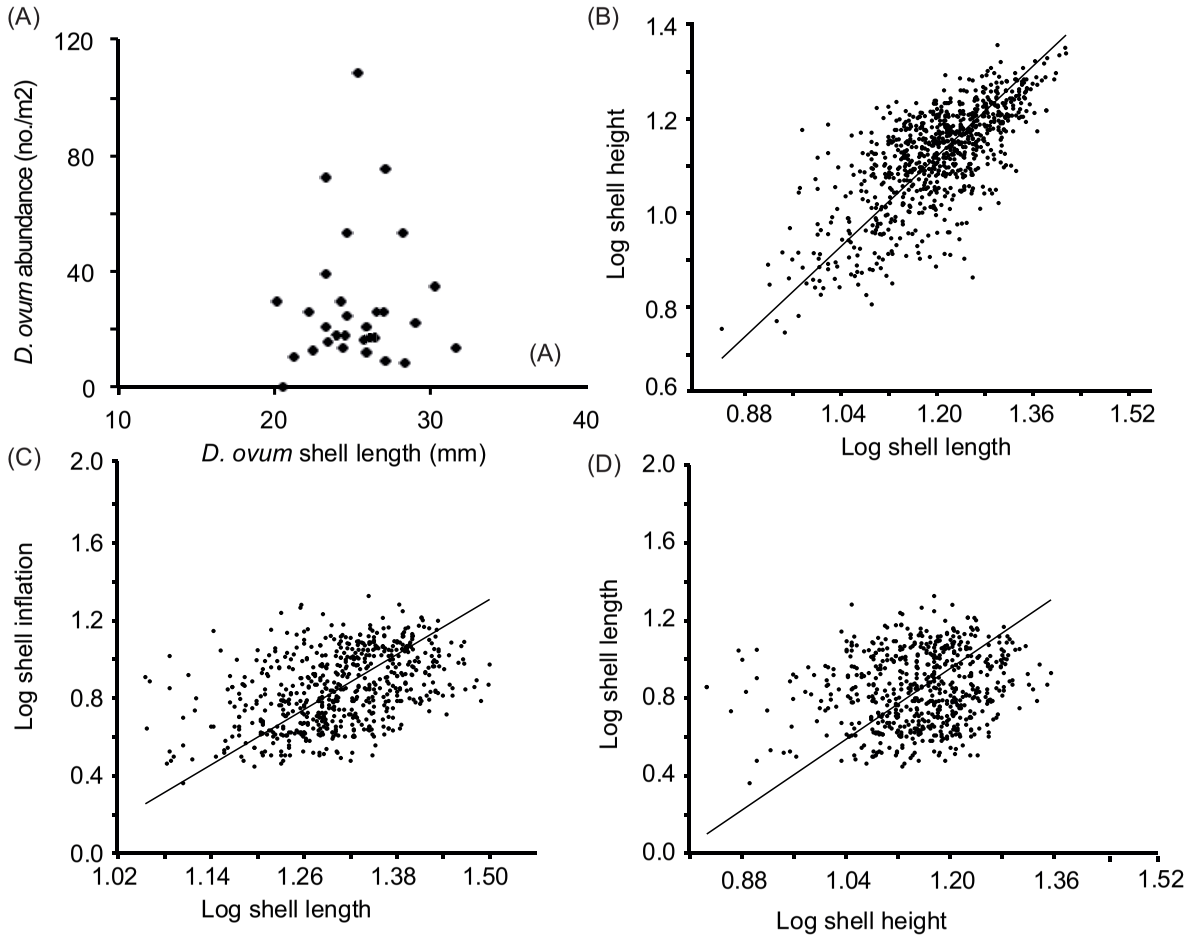

Fig. S2. (A) Dacryomya ovum shell length and abundance. (B) Reduced Mmjor axis regression of log shell length and log shell height. $R^2 = 0.48$, t = 27.89, $p<0.001$; a = 1.18. (C) Reduced major axis regression of log shell length and log shell inflation. $R^2=0.18$, t = 11.670 $p<0.001$, a = 0.43. (D) Reduced major axis regression of log shell height and log shell inflation. $R^2 = 0.03$, t = 4.0875, $p<0.001$, a = 2.28. When the allometric exponent 'a' of the relationship between *D. ovum* shell height and length is >1 there is positive allomtery between two variables.

©2020, Elsevier. This manuscript version is made available under the CC-BY-NC-ND 4.0 license http://creativecommons.org/licenses/by-nc-nd/4.0/

Supplementary information

Table S1. Preservation of *Dacryomya ovum* fossils from 30 stratigraphic heights sampled in the Alum Shales Member near Whitby, UK. The proportion of shells preserved as body fossils, internal and external moulds. The proportion of body fossils that were disarticulated single valves and those with some degree of fracturing are also shown.

Stratigraphic Height (m)	Body fossils (%)	Internal moulds (%)	External moulds (%)	Single valves (%)	Shells with fractures (%)	N
54.66	0	38	62	0	10	21
52.42	0	55	46	0	5	11
51.34	0	68	32	0	37	19
51.22	0	83	18	0	15	40
50.62	0	53	47	0	33	17
49.76	0	70	30	0	12	110
49.47	0	100	0	2	30	44
49.38	56	0	44	0	22	9
48.69	3	74	23	0	9	38
47.34	60	0	40	9	0	10
47.14	91	0	9	0	28	46
47.13	85	0	15	0	54	13
47.05	81	0	19	0	23	27
46.67	35	0	65	0	18	17
46.25	61	0	39	0	32	18
45.72	60	0	40	8	15	10
45.11	67	0	33	30	0	9
44.71	89	0	11	4	30	19
44.60	50	0	50	10	20	10
44.37	64	0	36	4	28	25
43.96	54	0	46	0	33	11
43.07	87	0	13	12	29	15
42.73	100	0	0	0	41	32
42.65	100	0	0	6	24	17
42.02	100	0	0	0	21	17
41.15	74	0	26	0	15	111
40.59	78	0	22	0	26	46
39.85	71	0	29	0	4	35
39.18	0	53	47	0	6	19
38.76	100	0	0	11	58	19

©2020, Elsevier. This manuscript version is made available under the CC-BY-NC-ND 4.0 license http://creativecommons.org/licenses/by-nc-nd/4.0/

Supplementary Table S2. Geological occurrences of the extinct bivalve *Dacryomya* at different geological sections, including the period, age, the lithostratigraphic position and facies in which they were found. (TRI = Triassic, Jur- Jurassic, and CRE = Cretaceous).

Species	Geographic locality	Period	Age	Lithostratigraphy	Facies	Reference
Dacryomya polaris Kiparisova	Olenek Bay, Siberia	TRI	Induan	Ulakhan-Krest Fm.	Mudstone	(Konstantinov et al. 2007)
Dacryomya skorochodi Kiparisova	East Laptev Sea coast, Siberia	TRI	Olenekian	Pastakh Fm.	Mudstone	(Konstantinov et al. 2013)
Dacryomya sp.	Buur River, Siberia	TRI	Olenekian	Teryutekh Fm.	Siltstone	(Konstantinov et al. 2013)
Dacryomya sp.	Chekurovskiy Cape, Lena River	TRI	late Olenekian	*Olenikites spiniplicatus* ammonoid zone	?	(Dagys and Ermakova 1988)
Dacryomya sp.	Khutuda-Yamu River, Russia	TRI	late Olenekian	Vostochnotaimyrskaya Fm.	Mudstone	(Dagys et al. 1996)
Dacryomya sp.	Zhitkov Cape, Primorye, Russia	TRI	late Olenekian	Zhitkov Fm.	Mud + Siltstone	(Zakharov et al. 2004)
Dacryomya sp.	Zhitkov Cape, Primorye, Russia	TRI	late Olenekian	Zhitkov Fm.	Calcareous Marl	(Zakharov et al. 2004)
Dacryomya sp.	Karangati Mountain, Olenek River, Siberia	TRI	early Anisian	*Grambergia taimyrensis* ammonoid zone	Mudstone	(Dagys et al. 1996)
Dacryomya sp.	Tsvetkov Cape, Russia	TRI	early Anisian	*Grambergia taimyrensis* ammonoid zone	?	(Dagys and Kurushin 1985)
Dacryomya sp.	Artist-Agatyn-Yurege Creek, Russia		early-middle Anisian	*Czekanowskites decipiens* ammonoid zone	Mudstone	(Dagys et al. 1996)
Dacryomya sp.	Schmidt Cape + Tchernyschev Bay, Primorye, Russia	TRI	Anisian	Karazin Fm.	Sandy Siltstone	(Zakharov et al. 2004)
Dacryomya sp.	Olenek Bay, Siberia	TRI	Anisian	Tuora-Khayata Fm.	Mudstone	(Konstantinov et al. 2013)
Dacryomya sp.	Republic of Sakha, Siberia	TRI	Anisian-Ladinian	Ystannakh Fm.	Siltstone	(Konstantinov et al. 2013)
Dacryomya sp.	Len Delta, Siberia	TRI	Ladinian	Ust'-Olenek Fm.	Mudstone	(Konstantinov et al. 2013)
Dacryomya sp.	Tsvetkov Cape, Russia	TRI	Ladinian	*Nathorstites mcconnelli* zone	Mudstone	(Dagys and Kurushin 1985)
Dacryomya sp.	Kotelny Island, Siberia	TRI	Carnian-Norian	Tikhaya River Fm.	Mudstone	(Konstantinov et al. 2013)
Dacryomya sp.	Surbel'akh River	TRI	Norian	Karadan Fm.	Silt + Mudstone	(Kazakov and Kurushin 1992)
Dacryomya sp.	Olenek Bay, Siberia	TRI	early-middle Norian	Tumul Fm.	Mudstone	(Konstantinov et al. 2013)

©2020, Elsevier. This manuscript version is made available under the CC-BY-NC-ND 4.0 license http://creativecommons.org/licenses/by-nc-nd/4.0/

Dacryomya sp.	Olenek River, Siberia	TRI	middle Norian	Tumul Fm.	Sandstone	(Kazakov and Kurushin 1992)

Species	**Geographic locality**	**Period**	**Age**	**Lithostratigraphy**	**Facies**	**Reference**
Dacryomya sp.	Olenek River, Siberia	TRI	Rhaetian	Tumul Fm.	Sandstone	(Kazakov and Kurushin 1992)
Dacryomya sp.	St Audrie's Bay, Somerset, England	TRI	Rhaetian	Westbury Fm.	Dark-grey Mudstone	(Mander et al. 2008)
Nuculana (Praesaccella) ovum (J de C Sowerby)	Umimmak Fjaeld, Greenland	JUR	Hettangian		Grey Sandstone	(Aberhan 1998b, Mander et al. 2008, Rosenkrantz 1934)
Dacryomya heberti (Martin)	St Audrie's Bay, Somerset, England	JUR	Hettangian-Pliensbachian	Blue Lias Fm.	Shale	(Hodges 2000)
Nuculana (Praesaccella) ovum	Graham Island, Tulsequah, Cry lake, British Columbia	JUR	Sinemurian-mid Toarcian	Takwahoni Fm., Graham Island Fm.	Siltstone + Shale	(Aberhan 1998a)
Dacryomya gaveyi Cox	Chipping Campden, Gloucestershire, UK	JUR	Pliensbachian		Shale	(Hodges 2000)
Nuculana (Praesaccella) ovum	South Neuquen, Argentina	JUR	Pliensbachian	Piedra-Pintada Fm.	Sandstone + fine tuffs	(Damborenea 1987)
Nuculana (Praesaccella) ovum	Quebrada Calquis, Quebrada Pinte, N Chile	JUR	Pliensbachian		Wackestone	(Aberhan 1992)
Nuculana (Praesaccella) ovum	Barranco de la Canada, Spain	JUR	early Toarcian	*Harpoceras serpentium ammonite* Zone	Marl	(Gahr 2002)
Nuculana (Praesaccella) ovum	Quebrada el Asiento, N Chile	JUR	Toarcian		Marl	(Aberhan 1992)
Nuculana (Praesaccella) ovum	South Neuquen, Argentina	JUR	Toarcian		Claystone	(Damborenea 1987)
Dacryomya lacryma	Causses, Southern France	JUR	Toarcian	Schistes Cartons	Bituminous Shale	(Fürsich et al. 2001)
Dacryomya ovum (J. de C Sowerby)	Holwell, Leicestershire, England	JUR	Toarcian	Whitby Mudstone Fm.	Mudstone	(Caswell and Coe 2012)
Dacryomya ovum	North Yorkshire, England	JUR	Toarcian	Whitby Mudstone Fm.	Mudstone	(Harries and Little 1999)
Dacryomya ovum	North Yorkshire, England	JUR	Toarcian	Blea Wyke Sandstone Fm.	Sandstone	(Fursich and Callomon 2004)
Dacryomya ovum	North Yorkshire, England	JUR	Toarcian	Whitby Mudstone Fm.	Mudstone	(Hesselbo and Jenkyns 1995, Little 1995, Martin 2004, Morris 1979, Rawson et al. 2000, Tate and Blake 1876, Wilson et al. 1934)
Dacryomya sp.	Taymyr, Russia	JUR	Toarcian	Kiterbyutsk Clay	Shale	(Nikitenko and Shurygin 1992, Zakharov et al. 2006)
Dacryomya sp.	Tyung River, Markha River, +	JUR	Toarcian	Timerdyakhskaya Fm.	Siltstone	(Shurygin 1983)

©2020, Elsevier. This manuscript version is made available under the CC-BY-NC-ND 4.0 license http://creativecommons.org/licenses/by-nc-nd/4.0/

	Vilyuy River, North Siberia					
Dacryomya inflata (Sowerby)	NW Siberia, NE Siberia, NE Russia	JUR	Toarcian	Togur + Kiterbyuk fms	Bituminous Shale	(Nikitenko et al. 2008)

Species	**Geographic locality**	**Period**	**Age**	**Lithostratigraphy**	**Facies**	**Reference**
Dacryomya sp.	Saratov, Siberia	JUR	early Aalenian-early Bathonian	Member III, Sokhur Quarry	Siltstone	(Meledina et al. 2005)
Dacryomya gigantea	Champ Island and Fiume Cape, Russia	JUR	early Aalenian	Fiume Fm.	Shale	(Basov et al. 2009, Nikitenko et al. 2008)
Dacryomya sp.	Caberfeidh Quarry, New Zealand	JUR	late Aalenian-early Bajocian	Purakauiti Fm.	Mudstone	(Gardner and Campbell 1997)
Dacryomya wiletti (Marwick)	Hinahina Quarry, New Zealand	JUR	late Aalenian-early Bajocian	Pounawea Fm.	Mudstone	(Gardner and Campbell 1997)
Dacryomya ovum	Hook Norton, England	JUR	Bathonian	Chipping Norton Fm.	Shale	(Horton and Edmonds 1987)
Dacryomya lacryma (J de C Sowerby)	Ler Kutch, Gujarat, West India.	JUR	Callovian	Athleta beds, Chari Fm.	Marl + Shale	(Agrawal and Kachhara 1979)
Dacryomya sp.	Iberian peninsula, Spain	JUR	Callovian-Kimmeridgian	Sot de Chera Fm.	Marl + Mudstone	(Delvene 2003)
Dacryomya sp.	South Tunisia	JUR	Callovian-Oxfordian	Tataouine Fm.	Packstone	(Holzapfel 1998)
Dacryomya acuta de Loriol	Wiltshire, UK	JUR	Oxfordian	Oxford Clay	Mudstone	(Martill and Hudson 1991)
Dacryomya roederi (de Loriol)	Ricla, Zaragova, Spain	JUR	late Oxfordian	Sot de Chera Fm.	Marl + Mudstone	(Delvene 2003)
Dacryomya sp.	Agan-Vakh area, W Siberia	CRE	early-mid Valanginian	Bazhenovo Fm.	Black shale	(Marinov et al. 2006)
Dacryomya chetaensis Sanin	Vostochno-Messoyakhskaya borehole 52, W Siberia	CRE	early Valanginian	Sukhaya Dudinka Fm.	Siltstone	(Marinov et al. 2015)

©2020, Elsevier. This manuscript version is made available under the CC-BY-NC-ND 4.0 license http://creativecommons.org/licenses/by-nc-nd/4.0/

References

Aberhan, M. 1992. Palokologie und zeitliche Verbreitung benthischer Faunengemeinschaften im Unterjura von Chile. Beringeria 5:1-174.

Aberhan, M. 1998a. Early Jurassic Bivalvia of western Canada. Part I Subclasses Palaeotaxodonta, Pteriomorphia and Isofilibranchia. Beringeria 21:57-150.

Aberhan, M. 1998b. Paleobiogeographic patterns of pectinoid bivalves and the Early Jurassic tectonic evolution of Western Canadian Terranes. Palaios 13(2):129-148.

Agrawal, S. K., and R. P. Kachhara. 1979. 1979. Habo Beds near Ler (Kutch): Pt. 3 - Biostratigraphy of the beds on the east of Ler. . Proceedings of the Indian National Science Academy (Part A) 45(2):129-146.

Basov, V. A., B. L. Nikitenko, and N. V. Kupriyanova. 2009. Lower–Middle Jurassic foraminiferal and ostracode biostratigraphy of the Barents Sea shelf. . Russian Geology and Geophysics 50(5):396-416.

Blott, S. J., and K. Pye. 2001. GRADISTAT: a grain size distribution and statistics package for the analysis of unconsolidated sediments. Earth Surface Processes and Landforms 26:1237-1248.

Caswell, B. A., and A. L. Coe. 2012. A high-resolution shallow marine record of the Toarcian (Early Jurassic) Oceanic Anoxic Event from the East Midlands Shelf, UK. Palaeogeography Palaeoclimatology Palaeoecology 365:124-135.

Dagys, A. S., A. A. Dagys, S. P. Ermakova, A. G. Konstantinov, N. I. Kurushin, E. S. Sobolev, and A. M. Truschelev. 1996. Triasovaya Fauna Severo-Vostoka Azii [Triassic fauna of North-Eastern Asia] (In Russian). Nauka, Novosibirisk.

Dagys, A. S., and S. P. Ermakova. 1988. Boreal'nye Pozdneolenekskie Ammonoidei Trudy Instituta Geologii i Geofiziki (Novosibirsk) 714:1-135.

Dagys, A. S., and N. I. Kurushin. 1985. Triasovye brakhiopody i dvustvorchatye mollyuski severa sredney Sibiri. Trudy Instituta Geologii i Geofiziki (Sibirskoe Otdelenie) 633:1-160.

Damborenea, S. E. 1987. Early Jurassic bivalvia of Argentina. Part 2: Superfamilies Pteriacea, buchiacea and part of Pectinacea. Palaeontographica Abteilung A 199(4-6):113-216.

Dean, W. E. 1974. Determination of carbonate and organic matter in calcareous sediments and sedimentary rocks by loss on ignition: Comparison with other methods. Journal of Sedimentary Petrology 44(242-248).

Delvene, G. 2003. Middle and Upper Jurassic bivalve associations from the Iberian Range (Spain). Geobios 36:519-531.

Fürsich, F. T., R. Berndt, T. Scheuer, and M. Gahr. 2001. Comparative ecological analysis of Toarcian (Lower Jurassic) benthic faunas from southern France and east-central Spain. Lethaia 34:169-199.

Fursich, F. T., and J. H. Callomon. 2004. Environments and faunal patterns in the Kachchh rift basin, Western India, during the Jurassic. . Rivista Italiana di Paleontologia e Stratigrafia 110:181-190.

Gahr, M. E. 2002. Palökologie des Makrobenthos im Unter-Toarc SW-Europas. Beringeria 31:3-204.

Gardner, R. N., and H. J. Campbell. 1997. The bivalve genus Grammatodon from the Middle Jurassic of the Catlins district, South Otago, New Zealand. New Zealand Journal of Geology and Geophysics 40 (4):487-498.

Harries, P. J., and C. T. S. Little. 1999. The early Toarcian (Early Jurassic) and the Cenomanian-Turonian (Late Cretaceous) mass extinctions: similarities and contrasts. Palaeogeography, Palaeoclimatology, Palaeoecology 154:39-66.

Hesselbo, S. P., and H. C. Jenkyns. 1995. A comparison of the Hettangian to Bajocian successions of Dorset and Yorkshire. Pp. 105-150. *In* P. D. Taylor, ed. Field Geology of the British Jurassic. Geological Society, London.

Hodges, P. 2000. The Early Jurassic Bivalvia from the Hettangian and lower Sinemurian of south-west Britain. Palaeontographical Society, London.

©2020, Elsevier. This manuscript version is made available under the CC-BY-NC-ND 4.0 license http://creativecommons.org/licenses/by-nc-nd/4.0/

Holzapfel, S. 1998. Palökologie benthischer Faunengemeinschaften und Taxonomie der Bivalven im Jura von Südtunesien. . Beringeria Würzburger geowissenschaftliche Mitteilungen 22:1-199.
Horton, A., and E. A. Edmonds. 1987. Geology of the country around Chipping Norton: memoir for 1: 50,000 geological sheet 218, new series (England and Wales) British Geological Survey.
Kazakov, A. M., and N. I. Kurushin. 1992. Stratigraphy of Norian and Rhaetian deposits in the northern Middle Siberia Russian Geology and Geophysics 33(6):1-8.
Konstantinov, A. G., E. S. Sobolev, and A. V. Yadrenkin. 2007. Detailed biostratigraphy of Triassic deposits in the Lena lower reaches (northern Yakutia). Russian Geology and Geophysics 48(9):721-736.
Konstantinov, A. G., E. S. Sobolev, and A. V. Yadrenkin. 2013. Triassic stratigraphy of the eastern Laptev Sea coast and New Siberian Islands. Russian Russian Geology and Geophysics 54(8):792-807.
Little, C. T. S. 1995. The Pliensbachian-Toarcian (Lower Jurassic) extinction event. PhD thesis. Bristol University, Bristol.
Mander, L., R. J. Twitchett, and M. J. Benton. 2008. Palaeoecology of the Late Triassic extinction event in the SW UK. Journal of the Geological Society, London 165:319-332.
Marinov, V. A., S. V. Meledina, O. S. Dzyuba, O. S. Urman, V. Yazikova, V. A. Luchinina, A. G. Zamirailova, and A. N. Fomin. 2006. Biofacies of Upper Jurassic and Lower Cretaceous sediments of central west Siberia. Stratigraphy and Geological Correlation 14(4):418-432.
Marinov, V. A., O. N. Zlobina, A. E. Igol'nikov, N. K. Mogucheva, and O. S. Urman. 2015. The biostratigraphy and sedimentary environments of the Lower Cretaceous section, Malaya Kheta structural-facies region, West Siberia. . Russian Geology and Geophysics 56 (10):1451-1460.
Martill, D. M., and J. D. Hudson. 1991. Fossils of the Oxford Clay. Palaeontological Association Field Guide to Fossils, number 4. The Palaeontological Association, London.
Martin, K. D. 2004. A re-evaluation of the realtionship between trace fossils and dysoxia. Geological Society London, Special Publications 228:141-156.
Meledina, S. V., B. N. Shurygin, and O. S. Dzyuba. 2005. Stages in development of mollusks, paleobiogeography of Boreal seas in the Early–Middle Jurassic and zonal scales of Siberia. Russian Geology and Geophysics 46(3):239-255.
Morris, K. A. 1979. A classification of Jurassic marine shale sequences: An example from the Toarcian (Lower Jurassic) of Great Britain. Palaeogeography Palaeoclimatology Palaeoecology 26:117-126.
Nikitenko, B., B. Shurygin, and M. Mickery. 2008. High resolution stratigraphy of the Lower Jurassic and Aalenian of Arctic regions as the basis for detailed palaeobiogeographic reconstructions. Norweigan Journal of Geology 88:267-278.
Nikitenko, B. L., and B. N. Shurygin. 1992. Lower Toarcian black shales and Pliensbachian-Toarcian crisis of the biota of Siberian paleoseas. Pp. 39-44. *In* D. E. Thurston, and K. Fujita, eds. 1992 Proceedings of the International Conference on Arctic Margins. U.S. Department of the Interior, Minerals Management Service, Alaska Outer Continental Shelf Region, Anchorage, Alaska.
Rawson, P. F., J. K. Wright, I. C. Starmer, F. Whitham, J. E. Hemingway, and J. T. Greensmith. 2000. The Yorkshire Coast (No. 34). . Geologists' Association, UK.
Rosenkrantz, A. 1934. The Lower Jurassic rocks of East Greenland. Meddrelelser om Grönland 110(1):1-56.
Shurygin, B. N. 1983. Toarskiye "Ledy" (Dacryomya) na severe Sibiri (Toarcian "Leda" (Dacryomya) of northern Siberia. Trudy Instituta Geologii i Geofiziki (Novosibirsk) 538:156-167.
Tate, R., and J. F. Blake. 1876. The Yorkshire Lias. John Van Voorst, London.
Wilson, V., J. E. Hemingway, and M. Black. 1934. A synopsis of the Jurassic rocks of Yorkshire. . Proceedings of the Geologists' Association 45(3):247-291.
Zakharov, V. A., B. N. Shurygin, V. I. Il'ina, and B. L. Nikitenko. 2006. Pliensbachian-Toarcian biotic turnover in north Siberia and the Arctic region. Stratigraphy and Geological Correlation 14(4):399-417.

©2020, Elsevier. This manuscript version is made available under the CC-BY-NC-ND 4.0 license http://creativecommons.org/licenses/by-nc-nd/4.0/

Zakharov, Y. D., A. M. Popov, and G. I. Buryi. 2004. Triassic Ammonoid succession in South Primorye: 3. Late Olenekian-Early Anisian Zones (*Neocolumbites insignis*, *Subcolumbites multiformis*, *Ussuriphyllites amurensis* and *Leiophyllites pradyumna*) . . Albertiana 31:54-64.

©2020, Elsevier. This manuscript version is made available under the CC-BY-NC-ND 4.0 license http://creativecommons.org/licenses/by-nc-nd/4.0/